

Successive Si–H/Si–C Bond Cleavage of Tertiary Silanes on Diruthenium Centers. Reactivities and Fluxional Behavior of the Bis(μ -silylene) Complexes Containing μ -Hydride Ligands[†]

Toshiro Takao, Masa-aki Amako, and Hiroharu Suzuki*

Department of Applied Chemistry, Graduate School of Science and Engineering, Tokyo Institute of Technology, and CREST, Japan Science and Technology Corporation (JST), 2-12-1 O-okayama, Meguro-Ku, Tokyo 152-8552, Japan

Received June 3, 2003

A series of μ -silylene complexes was synthesized by way of sequential Si–H and Si–C bond scission of tertiary silanes on diruthenium centers generated from $\text{Cp}^*\text{Ru}(\mu\text{-H})_4\text{RuCp}^*$ (**1**; $\text{Cp}^* = \eta^5\text{-C}_5\text{Me}_5$). While both bis- and mono(μ -diphenylsilylene) complexes, $\{\text{Cp}^*\text{Ru}(\mu\text{-SiPh}_2)(\mu\text{-H})\}_2$ (**3a**) and $\{\text{Cp}^*\text{Ru}(\mu\text{-H})\}_2(\mu\text{-SiPh}_2)$ (**4a**), were obtained in the case of Ph_3SiH , the reactions of **1** with Ph_2MeSiH and PhMe_2SiH exclusively afforded bis(μ -silylene) complexes, $\{\text{Cp}^*\text{Ru}(\mu\text{-SiPhMe})(\mu\text{-H})\}_2$ (**3b-syn/anti**) and $\{\text{Cp}^*\text{Ru}(\mu\text{-H})\}_2(\mu\text{-SiPhMe})(\mu\text{-SiMe}_2)$ (**3c**), respectively. The Si–C bond scission proceeded via prior π -coordination of the phenyl group of the intermediary formed silyl groups, which was supported by the fact that the reaction of **1** with $(\text{CH}_2=\text{CH})\text{RSiH}_2$ ($\text{R} = \text{Ph}, \text{Me}$) afforded exclusively the mono(μ -silylene) complex $\{\text{Cp}^*\text{Ru}(\mu\text{-H})\}_2(\mu\text{-SiEtR})$ (**4b**, $\text{R} = \text{Me}$; **4c**, $\text{R} = \text{Ph}$) as a result of intramolecular coordination of the vinyl group. Reaction of a mixture of **3b-syn** and **3b-anti** with PMe_3 afforded the bis(μ -silylene) complex $\{\text{Cp}^*\text{Ru}(\mu\text{-SiPhMe})\}_2(\text{PMe}_3)(\text{H})_2$ (**5**), which adopted only the syn structure with respect to the two bridging silylene ligands. Isomerization of the anti to the syn form arose from rotation of the bridging silylene ligands, which was confirmed by the VT-NMR studies of **3b-syn** and **3c**. While reactions of **3** with H_2 and CO afforded respectively the bis(μ -silyl) complexes $\{\text{Cp}^*\text{Ru}(\mu\text{-}\eta^2\text{-HSiR}_2)\}_2(\mu\text{-H})(\text{H})$ (**2**) and bis(μ -silylene) complexes containing two terminal carbonyl groups $\{\text{Cp}^*\text{Ru}(\text{CO})(\mu\text{-SiR}_2)\}_2$ (**6**), liberation of the bridging silylene ligand of **4** was observed during the reaction with H_2 and CO, together with formation of the mono(μ -silylene) complex $\{\text{Cp}^*\text{Ru}(\text{CO})\}_2(\mu\text{-CO})(\mu\text{-SiR}^1\text{R}^2)$ (**8a**, $\text{R}^1 = \text{R}^2 = \text{Ph}$; **8b**, $\text{R}^1 = \text{Me}, \text{R}^2 = \text{Et}$; **8c**, $\text{R}^1 = \text{Ph}, \text{R}^2 = \text{Et}$). X-ray diffraction studies were performed on **3c**, **4a,b**, **5**, and **8a,b**, and they clearly demonstrated the bridging silylene structures of these complexes.

Introduction

Reaction of organosilicon compounds with transition-metal complexes has been widely investigated in relation to silane polymerization,¹ hydrosilylation,² and redistribution at the silicon.³ Complexes obtained by oxidative addition of an Si–H bond are very important because they are considered to be key intermediates of such catalytic reactions. Many kinds of complexes having silicon ligands thus have been synthesized, which also revealed the ability of the silicon atom to attach to a metal center in various modes; for example,

silane, silyl, silylene, silylyne, silene, and disilene complexes are known.⁴

Among these categories, μ -silylene or μ -silyl complexes that have a bridging silicon ligand are one of the most widely investigated classes of silicon complexes.⁵ Reaction of a primary and a secondary silane with a mononuclear complex often afforded a dimeric product by successive oxidative addition of two Si–H bonds. For example, the monomeric manganese complex $(\eta^5\text{-C}_5\text{Me}_5)\text{Mn}(\text{CO})_3$ reacts with SiH_4 upon irradiation to generate the dimanganese complex $\{(\eta^5\text{-C}_5\text{Me}_5)\text{Mn}(\text{CO})(\text{H})\}_2(\mu\text{-SiH}_2)$.⁶ In this reaction, two Si–H bonds act as

[†] Dedicated with admiration and appreciation to Professor Akio Yamamoto and Dr. Nobuhiro Tamura, Technical director of the CREST project.

(1) Gauvin, F.; Harrod, J. F.; Woo, H.-G. *Adv. Organomet. Chem.* **1998**, *42*, 363–405.

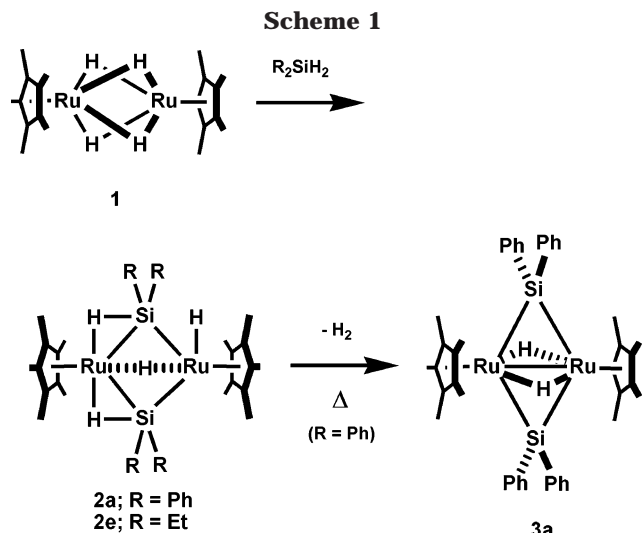
(2) For example: (a) Ojima, I. In *The Chemistry of Organic Silicon Compounds*; Patai, S., Rappoport, Z., Eds.; Wiley: New York, 1989; Chapter 25, pp 1479–1526. (b) Speier, J. L. *Adv. Organomet. Chem.* **1979**, *17*, 407–447.

(3) (a) Grumbine, S. K.; Tilley, T. D. *J. Am. Chem. Soc.* **1994**, *116*, 6951–6952. (b) Curtis, M. D.; Epstein, P. S. *Adv. Organomet. Chem.* **1981**, *19*, 213–255. (c) Kobayashi, T.; Hayashi, T.; Yamashita, H.; Tanaka, M. *Chem. Lett.* **1988**, 1411–1414.

(4) For example: (a) Shubert, U. *Adv. Organomet. Chem.* **1990**, *30*, 151–187. (b) Corey, J. Y.; Braddock-Wilking, J. *Chem. Rev.* **1999**, *99*, 175–292. (c) Aylett, B. J. *Adv. Inorg. Chem. Radiochem.* **1982**, *25*, 1–133. (d) Cundy, C. S.; Kingston, B. M.; Lappert, M. F. *Adv. Organomet. Chem.* **1973**, *11*, 253–330. (e) Tilley, T. D. In *The Chemistry of Organic Silicon Compounds*; Patai, S., Rappoport, Z., Eds.; Wiley: New York, 1989; Chapter 24, pp 1415–1478. (f) Zybilla, C.; Handwerker, H.; Friedrich, H. *Adv. Organomet. Chem.* **1994**, *36*, 229–281.

(5) Ogino, H.; Tobita, H. *Adv. Organomet. Chem.* **1998**, *42*, 223–290.

(6) Herrmann, W. A.; Voss, E.; Guggolz, E.; Ziegler, M. L. *J. Organomet. Chem.* **1985**, *284*, 47–57.



a clamp to bind two metal nuclei by oxidative addition. It has also been shown that reaction of a dinuclear complex with a secondary silane resulted in the formation of a bridging silicon ligand.^{7,8}

Thus far, many μ -silyl/silylene complexes have been synthesized in these ways, but most of them were studied only from an inorganic chemistry point of view. Although numerous structurally characterized complexes having a bridging silicon ligand are known, only quite limited studies of the reactivity have been done.^{8b,c,9,11} We previously reported that the bis(μ -silyl) complexes $\{\text{Cp}^*\text{Ru}(\mu\text{-}\eta^2\text{-HSiR}_2)\}_2(\mu\text{-H})(\text{H})$ (**2a**, R = Ph; **2e**, R = Et; $\text{Cp}^* = \eta^5\text{-C}_5\text{Me}_5$) were obtained by the reaction of the dinuclear ruthenium complex $\text{Cp}^*\text{Ru}(\mu\text{-H})_4\text{RuCp}^*$ (**1**) with R_2SiH_2 (R = Et, Ph) (Scheme 1).^{7a} It was revealed that two $2e\text{-}3c$ Ru–H–Si bonds were formed in bis(μ -silyl) complexes. The $2e\text{-}3c$ M–H–Si bond has been considered to be a frozen intermediate of the oxidative addition of an Si–H bond.^{4a,10} Actually, η^2 -coordinated Si–H bonds of **2a** underwent an oxidative addition reaction upon heating to yield the bis(μ -silylene) complex $\{\text{Cp}^*\text{Ru}(\mu\text{-SiPh}_2)(\mu\text{-H})_2$ (**3a**).^{7a}

(7) (a) Suzuki, H.; Takao, T.; Tanaka, M.; Moro-oka, Y. *J. Chem. Soc., Chem. Commun.* **1992**, 476–478. (b) Takao, T.; Yoshida, S.; Suzuki, H.; Tanaka, M. *Organometallics* **1995**, *14*, 3855–3868. (c) Ohki, Y.; Kojima, T.; Oshima, M.; Suzuki, H. *Organometallics* **2001**, *20*, 2654–2656.

(8) (a) McDonald, R.; Cowie, M. *Organometallics* **1990**, *9*, 2468–2478. (b) Wang, W.-D.; Eisenberg, R. *J. Am. Chem. Soc.* **1990**, *112*, 1833–1841. (c) Wang, W.-D.; Eisenberg, R. *Organometallics* **1992**, *11*, 908–912. (d) Carreño, C.; Riera, V.; Ruiz, M. A.; Jeannin, Y.; Philoche-Levisalles, M. *J. Chem. Soc., Chem. Commun.* **1990**, 15–17. (e) Fryzuk, M. D.; Rosenberg, L.; Rettig, S. J. *Organometallics* **1991**, *10*, 2537–2539. (f) Fryzuk, M. D.; Rosenberg, L.; Rettig, S. J. *Inorg. Chim. Acta* **1994**, *222*, 345–364. (g) Fryzuk, M. D.; Rosenberg, L.; Rettig, S. J. *Organometallics* **1996**, *15*, 2871–2880. (h) Rosenberg, L.; Fryzuk, M. D.; Rettig, S. J. *Organometallics* **1999**, *18*, 958–969. (i) Campion, B. K.; Heyn, R. H.; Tilley, T. D. *Organometallics* **1992**, *11*, 3918–3920. (j) Brittingham, K. A.; Gallaher, T. N.; Schreiner, S. *Organometallics* **1995**, *14*, 1070–1072. (k) Akita, M.; Hua, R.; Nakanishi, S.; Tanaka, M.; Moro-oka, Y. *Organometallics* **1997**, *16*, 5572–5584. (l) Kayser, B.; Eichberg, M. J.; Vollhardt, K. P. C. *Organometallics* **2000**, *19*, 2389–2392.

(9) (a) Corriu, R. J. P.; Moreau, J. J. E. *J. Chem. Soc., Chem. Commun.* **1980**, 278–279. (b) Carré, F. H.; Moreau, J. J. E. *Inorg. Chem.* **1982**, *21*, 3099–3105. (c) Horng, K. M.; Wang, S. L.; Liu, C. S. *Organometallics* **1991**, *10*, 631–635. (d) Corriu, R. J. P.; Lanneau, G. F.; Cjauhan, B. P. S. *Organometallics* **1993**, *12*, 2001–2003. (e) Wang, W.-D.; Eisenberg, R. *Organometallics* **1991**, *10*, 2222–2227. (f) Hashimoto, H.; Hayashi, Y.; Aratani, I.; Kabuto, C.; Kira, M. *Organometallics* **2002**, *21*, 1534–1536. (g) Hashimoto, H.; Aratani, I.; Kabuto, C.; Kira, M. *Organometallics* **2003**, *22*, 2199–2201.

(10) Crabtree, R. H. *Angew. Chem., Int. Ed. Engl.* **1993**, *32*, 789–805.

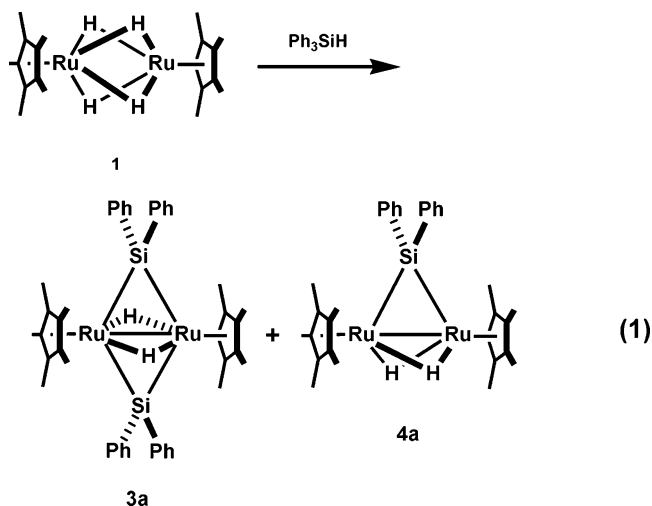
Cooperative action of the two ruthenium atoms was clearly represented in this reaction; one of the two ruthenium nuclei acts as a coordination site, and the other is an activation site. We will use the term *multimetallc activation* to refer to a distinctive manner of activation achieved by the concerted interaction among substrates and multiple metal centers. Recently, we reported another example of the bimetallic activation using vinylsilanes as substrates, in which it was shown that oxidative addition of an Si–C bond readily proceeded via formation of a $\mu\text{-}\eta^2\text{:}\eta^2\text{-vinylsilane}$ complex.^{11b} Although an Si–C bond was thought to be inert toward oxidative addition,¹² it was activated effectively by the cooperative action of two adjacent metal nuclei on the diruthenium system.

We describe herein a new example of bimetallic activation involving successive Si–H/Si–C(aryl) and Si–H/Si–C(sp³) bond cleavage. These reactions provided a new synthetic method of μ -silylene complexes using monohydrosilanes. Some reactions of the bis(μ -silylene) complex $\{\text{Cp}^*\text{Ru}(\mu\text{-SiR}_2)(\mu\text{-H})_2$ (**3**) and mono(μ -silylene) complex $\{\text{Cp}^*\text{Ru}(\mu\text{-H})_2(\mu\text{-SiR}_2)$ (**4**) with small molecules are also mentioned. Both complexes have a bridging divalent silicon ligand, and the structural data around the silicon, Ru–Si–Ru angles and Ru–Si distances, were similar to each other, but it was proved that their chemical properties are quite different. While ²⁹Si signals of mono(μ -silylene) complexes **4** appeared at a low magnetic field region (ca. δ 280 ppm) that was typical for a μ -silylene ligand,⁵ those of bis(μ -silylene) complexes **3** were observed at a considerably higher field region as the μ -silylene ligand (ca. δ 110 ppm). This implies that the bonding interaction between ruthenium and silicon is quite different in each compound, and this difference was reflected in the reactivities with small reactive molecules.

Results and Discussion

Reaction of $\text{Cp}^*\text{Ru}(\mu\text{-H})_4\text{RuCp}^*$ (**1**) with Ph_3SiH .

Reaction of the diruthenium tetrahydride complex $\text{Cp}^*\text{Ru}(\mu\text{-H})_4\text{RuCp}^*$ (**1**) with triphenylsilane yielded a mixture of the bis(μ -diphenylsilylene) complex $\{\text{Cp}^*\text{Ru}(\mu\text{-SiPh}_2)(\mu\text{-H})_2$ (**3a**) and the mono(μ -diphenylsilylene) complex $\{\text{Cp}^*\text{Ru}(\mu\text{-H})_2(\mu\text{-SiPh}_2)$ (**4a**) (eq 1). The ratio between **3a** and **4a** was dependent on the reaction conditions. Treatment of **1** with small excess amounts



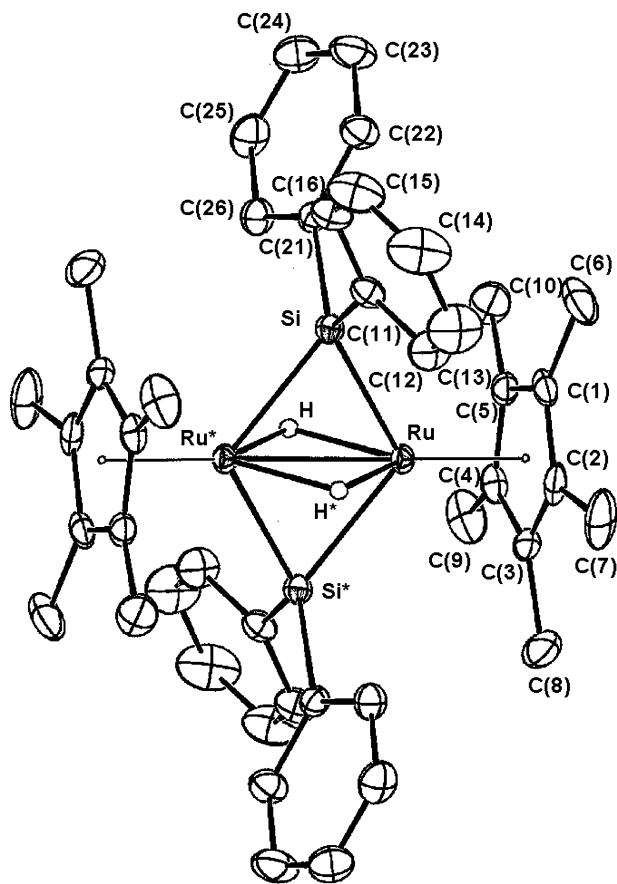


Figure 1. Molecular structure of $\{\text{Cp}^*\text{Ru}(\mu\text{-SiPh}_2)(\mu\text{-H})\}_2$ (**3a**), with thermal ellipsoids at the 30% probability level.

Table 1. Selected Bond Distances (Å) and Angles (deg) for 3a

Ru–Ru*	2.665(0)	Ru–H	1.72(3)
Ru–Si	2.364(1)	Ru–H*	1.73(3)
Ru–Si*	2.360(1)	Si–C(21)	1.885(2)
Si–C(11)	1.891(3)		
Si–Ru–Si*	111.30(3)	H–Ru–H*	79(1)
Ru–Si–Ru*	68.80(3)	C(11)–Si–C(21)	107.2(1)

of Ph₃SiH (3.0 equiv) afforded a mixture, in which the **3a**:**4a** ratio was estimated at 4:3. In contrast, when an equimolar amount of Ph₃SiH is slowly added dropwise to the solution of **1**, the **3a**:**4a** ratio changes to 1:5.

In the ¹H NMR spectrum of the mixture, two Cp* signals were observed at δ 1.40 and 1.59. The former signal was assignable to **3a**, which was independently synthesized by thermolysis of the bis(*μ*-diphenylsilyl) complex $\{\text{Cp}^*\text{Ru}(\mu\text{-}\eta^2\text{-HSiPh}_2)\}_2(\mu\text{-H})(\text{H})$ (**2a**).^{7a} Complex **3a** was already characterized and structurally determined by X-ray diffraction studies (Figure 1, Table 1). A singlet resonance of the hydrides of **3a** was observed at δ –19.70. Such a high-field shift around δ –20 is characteristic for the signal of hydride ligands of the bis(*μ*-silylene) complexes **3**.

The other Cp* signal observed at δ 1.59 was assignable to that of the mono(*μ*-diphenylsilylene) complex $\{\text{Cp}^*\text{Ru}(\mu\text{-H})\}_2(\mu\text{-SiPh}_2)$ (**4a**). The signal of the hydrides of **4a** was found at δ –13.51 as a singlet.

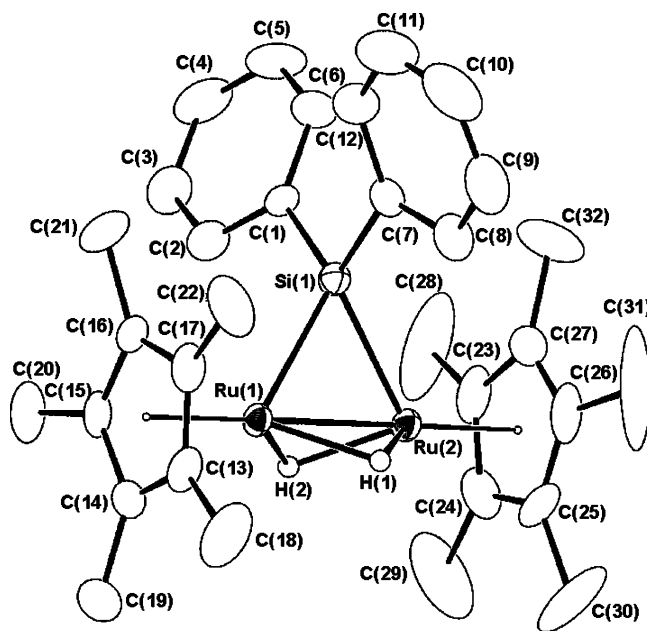


Figure 2. Molecular structure of $\{\text{Cp}^*\text{Ru}(\mu\text{-H})\}_2(\mu\text{-SiPh}_2)$ (**4a**), with thermal ellipsoids at the 30% probability level.

Table 2. Selected Bond Distances (Å) and Angles (deg) for 4a

Ru(1)–Ru(2)	2.4686(5)	Ru(1)–H(1)	1.86(5)
Ru(1)–Si(1)	2.3498(12)	Ru(1)–H(2)	1.80(7)
Ru(2)–Si(1)	2.3436(11)	Ru(2)–H(1)	1.83(5)
Si(1)–C(1)	1.884(5)	Ru(2)–H(2)	1.83(5)
Si(1)–C(7)	1.896(4)		
Ru(2)–Ru(1)–Si(1)	58.14(3)	H(1)–Ru(1)–H(2)	81(3)
Ru(1)–Ru(2)–Si(1)	58.39(3)	H(1)–Ru(2)–H(2)	79(3)
Ru(1)–Si(1)–Ru(2)	63.47(3)	C(1)–Si(1)–C(7)	108.6(2)

The solubility of both complexes, **3a** and **4a**, in organic solvents was quite low; thus, it was difficult to separate them as they were. While complex **3a** reacts with 1 atm of H₂ at ambient temperature to yield the bis(*μ*-silyl) complex **2a**, which is very soluble in pentane, complex **4a** does not react under those conditions. The mixture was converted to a mixture of **2a** and **4a** on exposure to 1 atm of H₂. Complex **4a**, then, was isolated in analytically pure form by rinsing with pentane. Complex **4a** was fully characterized on the basis of ¹H, ¹³C, and ²⁹Si NMR, IR, and FD-MS spectral data as well as analytical data. The structure of **4a** was determined by X-ray diffraction studies using a single crystal obtained from a diluted cold CH₂Cl₂ solution.

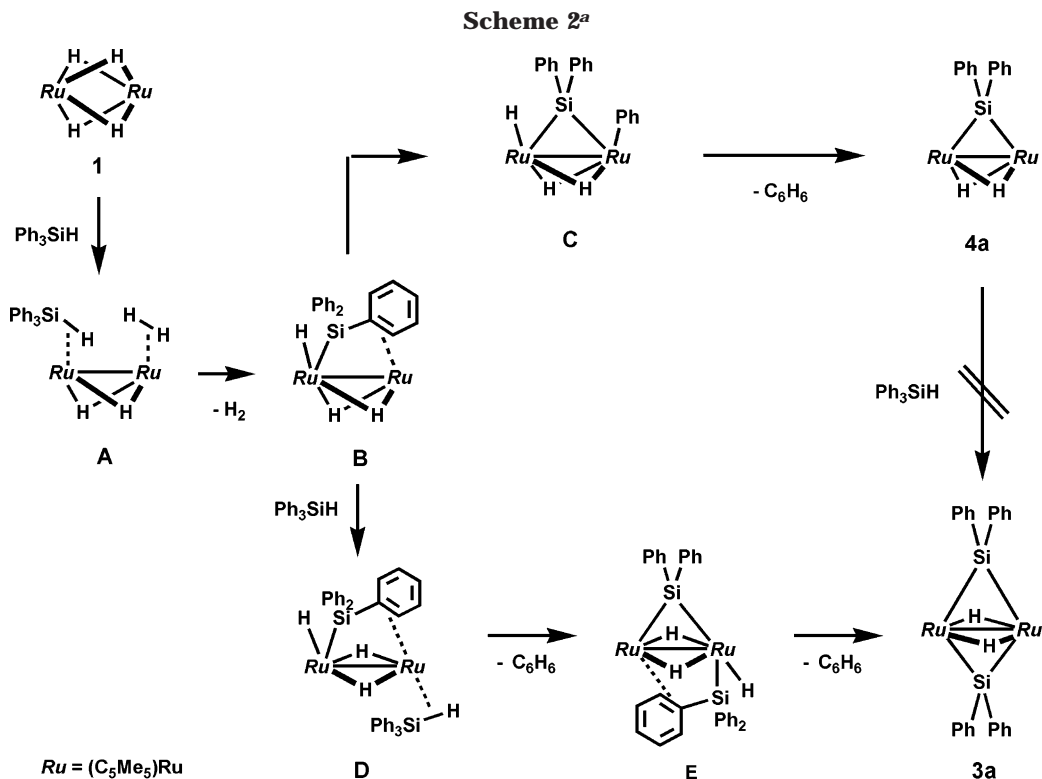
The molecular structure of **4a** is shown in Figure 2, which clearly demonstrates the dinuclear structure bridged by a silicon atom. Hydride ligands bonded to ruthenium atoms were located during sequential difference Fourier syntheses and were refined isotropically. The crystal data for **4a** are given in the Experimental Section (Table 8), and selected bond lengths and angles are given in Table 2.

The Ru(1)–Ru(2) distance, 2.4686(5) Å, was similar to that of **1** (2.4630(5) Å)¹³ and considerably shorter than that of **3a** (2.665(0) Å).^{7a} The Ru–Ru distance of 2.46 Å corresponds to that of a triple bond between two

(11) (a) Takao, T.; Suzuki, H.; Tanaka, M. *Organometallics* **1994**, *13*, 2554–2556. (b) Takao, T.; Amako, M.; Suzuki, H. *Organometallics* **2001**, *20*, 3406–3422.

(12) Sakaki, S.; Ieki, M. *J. Am. Chem. Soc.* **1993**, *115*, 2373–2381.

(13) (a) Suzuki, H.; Omori, H.; Lee, D.-H.; Yoshida, Y.; Moro-oka, Y. *Organometallics* **1988**, *7*, 2243–2245. (b) Suzuki, H.; Omori, H.; Lee, D.-H.; Yoshida, Y.; Fukushima, M.; Tanaka, M.; Moro-oka, Y. *Organometallics* **1984**, *13*, 1129–1146.



^a $Ru = (C_5Me_5)Ru$.

ruthenium nuclei, and a triple bond makes each ruthenium coordinatively saturated according to the EAN rule. An ab initio MO calculation of **1**, however, suggested that there was no bonding interaction between two ruthenium atoms.¹⁴ It was concluded in this paper that the Ru–Ru distance was shortened as a result of ligation of the four hydrides in the bridging mode, which bound two ruthenium nuclei strongly. Though concrete evidence for an Ru–Ru bonding interaction is lacking at present, the very acute Ru(1)–Si–Ru(2) angle (63.49(4)°) implies that there would be a strong interaction between two ruthenium atoms.¹⁵

The Ru–Si distances (2.3498(12), 2.3436(11) Å) lie in the range of the reported values for Ru–Si σ -bond lengths (2.288(11)–2.507(8) Å)^{4b} and were nearly equal to those of **3a** (average 2.36 Å). Although there was no distinct difference in the Ru–Si distances between **3a** and **4a**, their magnetic environment was proved to be considerably different by means of ²⁹Si NMR spectroscopy. The ²⁹Si signals of **3a** and **4a** appeared at δ 109.8 and 265.0, respectively. It has been noted that the chemical shift of a silicon ligand depends on various factors, such as electron negativity of the substituent, coordination number, p_π – d_π and, d_π – d_π interactions, and so on.¹⁶ Thus, it seems to be difficult to predict the coordination mode of a silicon atom only on the basis of the chemical shift such as ¹H and ¹³C NMR. Indeed, it was known that ²⁹Si signals of μ -silyl/silylene complexes

appeared in a very wide range (δ 59.5–289.1).⁵ In this case, however, since both **3a** and **4a** have the same substituents on the bridging silicon and their Ru–Si σ -bond distances were nearly the same, the chemical shift of the ²⁹Si NMR spectra probably reflects the difference in their bonding interaction, which is discussed later.

It is obvious that the μ -silylene complexes **3a** and **4a** were formed as a result of Si–C(aryl) bond cleavage of Ph₃SiH. The phenyl group was eliminated as benzene, and generation of benzene was confirmed by means of GC-MS. Neither biphenyl nor diphenylsilane was formed. Such Si–C(aryl) bond cleavage would be achieved by the concerted interaction of the two adjacent ruthenium atoms. The reaction was monitored by means of ¹H NMR, but no detectable intermediate was observed during the reaction. Generation of dihydrogen was confirmed by the singlet observed at δ 4.51. Akita et al. also reported Si–C(aryl) bond cleavage by the reaction of the diruthenium complex {CpRu(μ -CH₂)₂(CO)(MeCN)} (Cp = η^5 -C₅H₅) with Ph₃SiH to yield a μ -silylene complex.^{8k} The Si–C(aryl) bond cleavage of triphenylsilane most likely proceeds via formation of the μ -triphenylsilane intermediates **B** and **E** shown in Scheme 2. Intramolecular coordination of a vinyl group of a dimethylvinylsilane in the μ - η^2 : η^2 -dimethylvinylsilane complex {Cp*Ru(μ -H)}₂{ μ - η^2 : η^2 -HSiMe₂(CH=CH₂)} was confirmed by means of the X-ray diffraction studies, which can be regarded as a model compound of intermediate **B** in Scheme 2.^{11b} A P–C bond of PPh₃ was also cleaved by the tetrahydride complex **1** at ambient temperature, which afforded the μ -phosphido complex (Cp*Ru)₂(μ -PPh₂)(μ - η^2 : η^2 -C₆H₆)(μ -H).¹⁷

(14) Koga, N.; Morokuma, K. *J. Mol. Struct.* **1993**, *300*, 181–189.

(15) (a) Coleman, J. M.; Dahl, L. F. *J. Am. Chem. Soc.* **1967**, *89*, 542–552. (b) Stevenson, D. L.; Dahl, L. F. *J. Am. Chem. Soc.* **1967**, *89*, 3721–3726. (c) Dahl, L. F.; De Gil, E. R.; Feltham, R. D. *J. Am. Chem. Soc.* **1969**, *91*, 1653–1654. (d) Connelly, N. G.; Dahl, L. F. *J. Am. Chem. Soc.* **1970**, *92*, 7470–7472. (e) Connelly, N. G.; Dahl, L. F. *J. Am. Chem. Soc.* **1970**, *92*, 7472–7474.

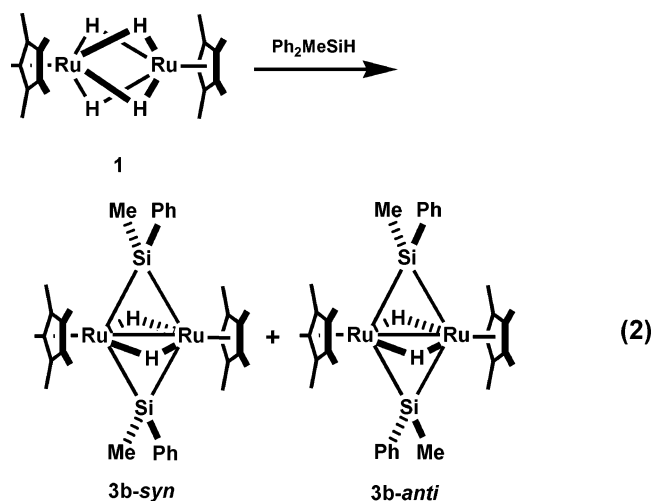
(16) Williams, E. A. In *The Chemistry of Organic Silicon Compounds*; Patai, S., Rappoport, Z., Eds.; Wiley: New York, 1989; Chapter 8, pp 511–554.

(17) Omori, H.; Suzuki, H.; Take, Y.; Moro-oka, Y. *Organometallics* **1989**, *8*, 2270–2272.

Complex **4a** did not react with Ph₃SiH at ambient temperature. This fact strongly indicates that bis(μ -silylene) complex **3a** was not produced via **4a**, and it is noteworthy that **3a** and **4a** were formed via independent paths. Triphenylsilane is so large that coordination of the second molecule of Ph₃SiH was suppressed by its steric demand. Coordination of an Si–H bond of the second molecule would compete with intramolecular coordination of the phenyl group. Such suppression by the intramolecular coordination is clearly seen in the reaction of **1** with the secondary vinylsilane (CH=CH₂)–RSiH₂ (vide infra).

Reaction of Cp*Ru(μ -H)₄RuCp* with Ph₂MeSiH.

The reaction of **1** with 2 molar equiv of diphenylmethylsilane afforded a mixture of two diastereomers of the bis(μ -silylene) complex {Cp*Ru(μ -SiPhMe)(μ -H)}₂ (**3b-syn** and **3b-anti**) with respect to the orientation of the substituents at the bridging silicons (eq 2). The ratio



between **3b-syn** and **3b-anti** was estimated at 55:45 by ¹H NMR spectroscopy. Although the syn/anti ratio did not seemingly change in the temperature range from –50 to 70 °C, it was considered that the ratio was determined thermodynamically rather than kinetically. Reaction of the syn and anti mixture of **3b** with trimethylphosphine resulted in exclusive formation of the syn isomer, and elimination of the coordinated PMe₃ resulted in re-formation of the syn and anti mixture of **3b** (vide infra). This result implied equilibrium between **3b-syn** and **3b-anti**. In addition, rotation of the bridging silylene ligand within the NMR time scale was clearly shown in the VT-NMR studies of the mixed-bridge bis(μ -silylene) complex {Cp*Ru(μ -H)}₂(μ -SiMe₂)(μ -SiPhMe) (**3c**; vide infra).

Unlike the reaction of **1** with Ph₃SiH, the mono(μ -silylene) complex was not obtained at all, even in the reaction with less than 2 molar equiv of Ph₂MeSiH. This is probably due to the smaller steric bulk of Ph₂MeSiH than that of Ph₃SiH.

In this reaction, Si–C(aryl) bond cleavage of Ph₂MeSiH predominated over Si–C(sp³) bond cleavage. Si–C(sp³) bond cleavage to form a μ -SiPh₂ bridge did not take place. Preference of Si–C(aryl) bond cleavage over that of the Si–C(sp³) bond has been also observed in the thermolysis of the diplatinum silyl complex {Pt(PR₃)(SiPhMe₂)(μ -H)}₂ (R = C₆H₁₁), which resulted in

the exclusive formation of {Pt(PR₃)(μ -SiMe₂)(μ -H)}₂.¹⁸ Judging from these reactions, oxidative addition of an Si–C(aryl) bond is more preferable than that of an Si–C(sp³) bond. This preference was most likely due to the ability of the phenyl group to engage in η^2 coordination to the neighboring metal center, and η^2 coordination would facilitate the Si–C(aryl) bond cleavage. Such bond cleavage assisted by η^2 coordination of a phenyl group has appeared in earlier papers.¹⁹

Although complexes **3b-syn** and **3b-anti** were not separated from each other, they were characterized on the basis of ¹H, ¹³C, and ²⁹Si NMR spectra and FD-MS spectra of the mixture. In the ¹H NMR spectra of the mixture measured at –40 °C, three resonances for the hydride ligands were observed. A singlet observed at δ –20.44 was assignable to the hydride signal of **3b-anti**, and two doublets observed at δ –21.01 (J_{H-H} = 6.1 Hz) and –19.77 (J_{H-H} = 6.1 Hz) were assignable to those of **3b-syn**. Although the signals assignable to **3b-anti** did not show any broadening even in the higher temperature region, the hydride signals of **3b-syn** coalesced into one signal at 20 °C. However, the shape of Cp* and methyl proton signals of **3b-syn** did not change upon warming. These results show that the site-exchange process of the hydride ligands occurs in the bis(μ -silylene) complexes. Activation parameters of this fluxional process were estimated at ΔH^\ddagger = 16.7 \pm 0.4 kcal mol^{–1} and ΔS^\ddagger = 12.5 \pm 1.6 cal mol^{–1} K^{–1}. Mechanistic studies of the fluxional processes are discussed in detail later.

Although hydride signals of **3b-anti** were not dependent on temperature, the two hydride ligands in **3b-anti** likely exchange as those observed in **3b-syn**. Since **3b-anti** adopts a C₂-symmetrical structure with respect to the Ru–Ru axis, two hydride ligands are always kept in magnetic equivalence. Therefore, the site-exchange process would not appear in the NMR signals of **3b-anti**. This feature is also applied to the bis(μ -diphenylsilylene) complex **3a**, which has a D_{2h} structure.

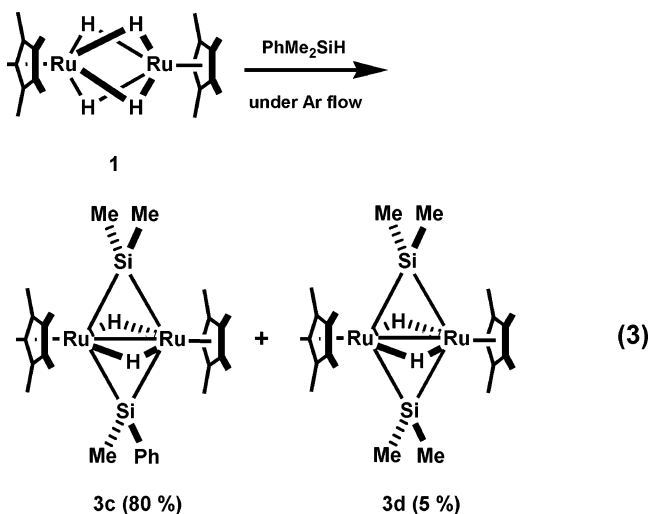
Reaction of Cp*Ru(μ -H)₄RuCp* with PhMe₂SiH. While Si–C(sp³) bond cleavage of Ph₂MeSiH was not observed as mentioned above, Si–C(sp³) bond scission of PhMe₂SiH occurred in the reaction of **1** with PhMe₂SiH. Treatment of **1** with 2 molar equiv of PhMe₂SiH afforded a mixture of the mixed-bridge bis(μ -silylene) complex {Cp*Ru(μ -H)}₂(μ -SiPhMe)(μ -SiMe₂) (**3c**) and the bis(μ -silyl) complex (Cp*Ru)₂(μ - η^2 -HSiPhMe)(μ - η^2 -HSiMe₂)(μ -H)(H) (**2c**). Small amounts of {Cp*Ru(μ -SiMe₂)(μ -H)}₂ (**3d**) and {Cp*Ru(μ - η^2 -HSiMe₂)}₂(μ -H)(H) (**2d**), which were formed as a result of two Si–C(aryl) bond scissions, were also observed in the mixture

(18) (a) Ciriano, M.; Gree, M.; Howard, J. A. K.; Proud, J.; Spencer, J. L.; Stone, F. G. A.; Tsipis, C. A. *J. Chem. Soc., Dalton Trans.* **1978**, 801–808. (b) Auburn, M.; Ciriano, M.; Howard, J. A. K.; Murray, M.; Pugh, N. J.; Spencer, J. L.; Stone, F. G. A.; Woodward, P. *J. Chem. Soc., Dalton Trans.* **1980**, 659–666.

(19) (a) Jones, W. D.; Feher, F. J. *J. Am. Chem. Soc.* **1986**, *108*, 4814–4819. (b) Jones, W. D.; Feher, F. J. *J. Am. Chem. Soc.* **1985**, *107*, 620–631. (c) Jones, W. D.; Feher, F. J. *Inorg. Chem.* **1984**, *23*, 2376–2388. (d) Jones, W. D.; Feher, F. J. *J. Am. Chem. Soc.* **1984**, *106*, 1650–1663. (e) Jones, W. D.; Feher, F. J. *Organometallics* **1983**, *2*, 686–687. (f) Jones, W. D.; Feher, F. J. *J. Am. Chem. Soc.* **1982**, *104*, 4240–4242. (g) Belt, S. T.; Duckett, S. B.; Helliwell, M.; Perutz, R. N. *J. Chem. Soc., Chem. Commun.* **1989**, 928–930. (h) Belt, S. T.; Dong, L.; Duckett, S. B.; Jones, W. D.; Partridge, M. G.; Perutz, R. N. *J. Chem. Soc., Chem. Commun.* **1991**, 266–269. (i) Chin, R. M.; Dong, L.; Duckett, S. B.; Partridge, M. G.; Jones, W. D.; Perutz, R. N. *J. Am. Chem. Soc.* **1993**, *115*, 7685–7695.

(determined by the FD-MS spectra of the crude mixture).

The bis(μ -silyl) complex **2c** was formed by the reaction of **3c** with liberated dihydrogen during the reaction of **1** with PhMe_2SiH . The reaction of bis(μ -silylene) complex **3** with dihydrogen to yield the bis(μ -silyl) complex **2** is described later. Therefore, it was required to remove dihydrogen to raise the selectivity of **3c**. The yield of **3c** increased up to 80% by bubbling argon to remove H_2 from the solution (determined by the ^1H NMR) (eq 3). The yield of **3d** was estimated at 5% on the basis of



the ^1H NMR spectra. Analytically pure **3c** was obtained by recrystallization from cold pentane solution. Complex **3c** was fully characterized on the basis of ^1H , ^{13}C , and ^{29}Si NMR, IR, and FD-MS spectra.

In the ^1H NMR spectra of **3c**, a singlet assignable to the Cp^* groups was observed at δ 1.65. At -60°C , three singlet signals assignable to the methyl groups on the bridging silicon atoms were observed at δ 0.97, 0.79, and 0.74, respectively. Resonance for the phenyl group of **3c** was found at between δ 7.7 and 6.7. Observation of these three methyl signals and one phenyl group shows the mixed-bridge structure of **3c**. Two doublets of the hydride ligands were observed at δ -20.44 (d, $J_{\text{H-H}} = 6.0$ Hz) and -21.13 (d, $J_{\text{H-H}} = 6.0$ Hz), which coalesced into one signal at -5°C . This indicated that an intramolecular site-exchange process of the hydride ligands occurred in **3c**. Activation parameters for the fluxional process were estimated at $\Delta H^\ddagger = 16.4 \pm 0.7$ kcal mol $^{-1}$ and $\Delta S^\ddagger = 15.5 \pm 2.6$ cal mol $^{-1}$ K $^{-1}$. These were very similar to those of **3b-syn** ($\Delta H^\ddagger = 16.7 \pm 0.4$ kcal mol $^{-1}$ and $\Delta S^\ddagger = 12.5 \pm 1.6$ cal mol $^{-1}$ K $^{-1}$).

Since the yield of **3d** was very low and isolation of **3d** was difficult, spectral data of **3d** were not fully obtained. It was characterized on the basis of the ^1H NMR spectra and FD-MS analysis of the mixture. A nonfluxional singlet signal of the hydride observed at δ -21.16 , which is typical for the bis(μ -silylene) complexes **3**, implied the highly symmetrical structure of **3d**. The FD-MS analysis of the crude products was quite consistent with the existence of two μ - SiMe_2 bridges in **3d**.

In addition to the site-exchange process of the hydride ligands, coalescence of the methyl protons of the μ - SiMe_2 group was observed at higher temperature. While the shape of the methyl signal observed at δ 0.97 that was

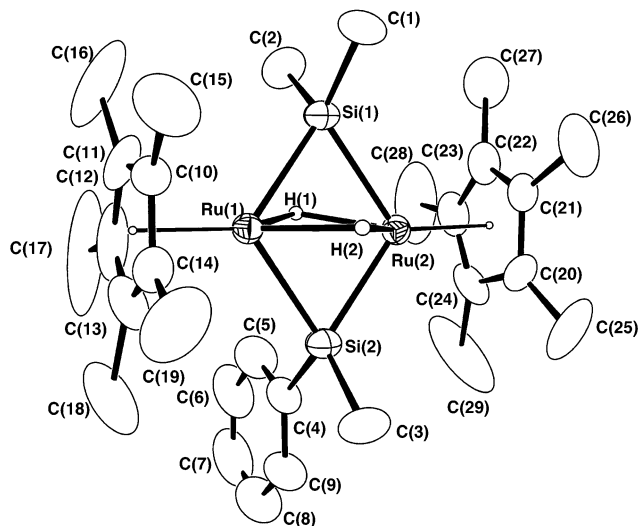


Figure 3. Molecular structure of $\{\text{Cp}^*\text{Ru}(\mu\text{-H})_2(\mu\text{-SiPhMe})(\mu\text{-SiMe}_2)\}$ (**3c**), with thermal ellipsoids at the 30% probability level.

Table 3. Selected Bond Distances (Å) and Angles (deg) for **3c**

Ru(1)–Ru(2)	2.6617(10)	Ru(3)–Ru(4)	2.6652(10)
Ru(1)–Si(1)	2.355(2)	Ru(3)–Si(3)	2.364(2)
Ru(1)–Si(2)	2.353(2)	Ru(3)–Si(4)	2.3528(19)
Ru(1)–H(1)	1.7744(7)	Ru(3)–H(3)	1.9146(6)
Ru(1)–H(2)	1.8811(6)	Ru(3)–H(4)	1.7367(7)
Ru(2)–Si(1)	2.360(2)	Ru(4)–Si(3)	2.363(2)
Ru(2)–Si(2)	2.345(2)	Ru(4)–Si(4)	2.3568(19)
Ru(2)–H(1)	1.7717(6)	Ru(4)–H(3)	1.7778(7)
Ru(2)–H(2)	1.8437(7)	Ru(4)–H(4)	1.8297(6)
Si(1)–C(1)	1.899(8)	Si(3)–C(30)	1.893(7)
Si(1)–C(2)	1.888(9)	Si(3)–C(31)	1.883(7)
Si(2)–C(3)	1.884(7)	Si(4)–C(32)	1.878(7)
Si(2)–C(4)	1.895(8)	Si(4)–C(33)	1.876(7)
Ru(2)–Ru(1)–Si(1)	55.72(5)	Ru(4)–Ru(3)–Si(3)	55.67(5)
Ru(2)–Ru(1)–Si(2)	55.34(5)	Ru(4)–Ru(3)–Si(4)	55.60(5)
Si(1)–Ru(1)–Si(2)	110.99(7)	Si(3)–Ru(3)–Si(4)	111.20(7)
Ru(1)–Ru(2)–Si(1)	55.54(5)	Ru(3)–Ru(4)–Si(3)	55.70(5)
Ru(1)–Ru(2)–Si(2)	55.62(5)	Ru(3)–Ru(4)–Si(4)	55.46(5)
Si(1)–Ru(2)–Si(2)	111.08(7)	Si(3)–Ru(4)–Si(4)	111.10(7)
Ru(1)–Si(1)–Ru(2)	68.74(6)	Ru(3)–Si(3)–Ru(4)	68.63(5)
C(1)–Si(1)–C(2)	105.6(5)	C(30)–Si(3)–C(31)	103.5(4)
Ru(1)–Si(2)–Ru(2)	69.03(6)	Ru(3)–Si(4)–Ru(4)	68.93(5)
C(3)–Si(2)–C(4)	107.4(4)	C(32)–Si(4)–C(33)	106.1(4)

assignable to the methyl group of the μ - SiPhMe bridge did not change at any temperature, the signals observed at δ 0.79 and 0.74 coalesced into one signal at 90°C . Activation parameters for the dynamic process were estimated at $\Delta H^\ddagger = 16.5 \pm 0.7$ kcal mol $^{-1}$ and $\Delta S^\ddagger = -7.8 \pm 2.1$ cal mol $^{-1}$ K $^{-1}$ by means of the line-shape analysis. These parameters are considerably different from those of the hydride site-exchange process, which implies that these fluxional processes occur independently.

X-ray diffraction studies were carried out using a red single crystal of **3c**. An ORTEP diagram of **3c** is depicted in Figure 3, and selected bond distances and angles are listed in Table 3. The structure clearly shows the μ - SiPhMe bridge formed via $\text{Si}-\text{C}(\text{sp}^3)$ bond cleavage. Since there were two independent molecules in the unit cell, one of them was represented.

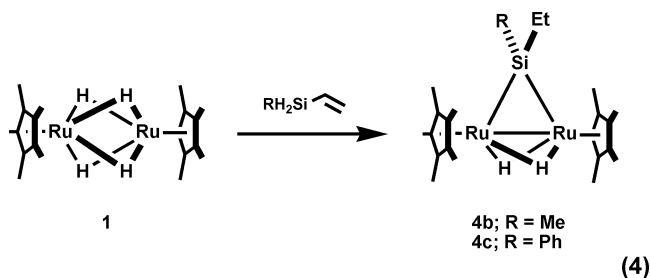
The Ru–Ru distance of 2.663 Å (av) is similar to that of **3a** and implies existence of an Ru=Ru double bond. Ru–Si lengths are also the same as those of **3a** and lie

in the range of Ru–Si single-bond lengths. The acute Ru–Si–Ru angles indicate strong interaction between two ruthenium atoms, which was also observed in **3a**.¹⁵

Cleavage of an Si–C(aryl) bond proceeds more readily than that of an Si–C(sp³) bond due to prior π -coordination through the aryl group. Indeed, in the reaction of **1** with Ph₂MeSiH, Si–C(aryl) bond scission took place with 100% selectivity. While the dimethylsilylene bridge of **3c** was formed via Si–C(aryl) bond cleavage, the phenylmethylsilylene bridge was apparently formed via Si–C(sp³) bond cleavage, which was seemingly unfavorable. A similarly curious preference was also seen in the reaction of a μ -di-*tert*-butyl silane complex with diethylsilane to yield the bis(μ -silyl) complex (Cp*Ru)₂(μ - η^2 -HSi^tBu₂)(μ - η^2 -HSiEtH)(μ -H)(H) (**2e**);^{7b} Si–C(sp³) bond cleavage took precedence over that of the Si–H bond. The reason for the exclusive Si–C(sp³) bond cleavage is still unclear, but these Si–C bond cleavages were only achieved by the cooperative effect of the adjacent ruthenium centers.

Complex **1** did not react with phenyltrimethylsilane, which has no Si–H bond. This indicates that initial interaction of an Si–H bond to a ruthenium center was essential for these Si–C bond cleavages. This result implied the path of multimetallic activation and the importance of the adjacent metal centers for activating the Si–C bonds.

Reaction of Cp*Ru(μ -H)₄RuCp* with R(CH₂=CH)SiH₂ (R = Me, Ph). In the reaction of **1** with secondary silane, such as Ph₂SiH₂ and Et₂SiH₂, 2 molar equiv of silane was consumed to form the bis(μ -silyl) complex {Cp*Ru(μ - η^2 -HSiR₂)}₂(μ -H)(H) (**2a**, R = Ph; **2e**, R = Et).^{7a} In contrast, the reaction with the second silane molecule was suppressed due to the intramolecular coordination of the substituents on the silane in the case that the silane contained substituents having coordination ability to a metal center. Treatment of **1** with the dihydrovinylsilane R(CH₂=CH)SiH₂ resulted in the exclusive formation of the mono(μ -silylene) complex {Cp*Ru(μ -H)}₂(μ -SiREt) (**4b**, R = Me; **4c**, R = Ph; eq 4). Complexes **4b,c** were isolated in analytically



pure form by rinsing with pentane and fully characterized on the basis of ¹H, ¹³C, and ²⁹Si NMR and IR spectral data as well as analytical data.

In the ¹H NMR spectrum of **4b**, a singlet signal assignable to methyl protons of the Cp* groups was observed at δ 1.77. Two doublets of hydride ligands were observed at δ -14.60 (d, $J_{\text{H-H}} = 3.7$ Hz) and -14.69 (d, $J_{\text{H-H}} = 3.7$ Hz), respectively. A couple of a quartet and a triplet assignable to an ethyl group on the bridging silicon atom was observed at δ 1.43 (q, $J_{\text{H-H}} = 7.7$ Hz) and 1.71 (t, $J_{\text{H-H}} = 7.7$ Hz), respectively.

The ²⁹Si signal of **4b** (Me, Et) was observed at an extremely low-field region (δ 310.8). Such a large

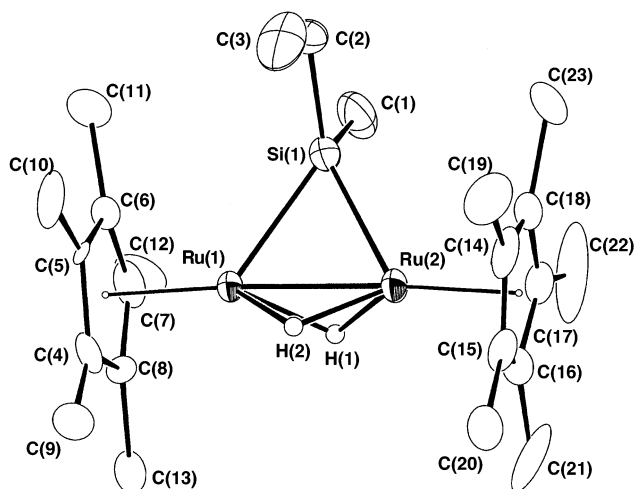


Figure 4. Molecular structure of {Cp*Ru(μ -H)}₂(μ -SiMeEt) (**4b**), with thermal ellipsoids at the 30% probability level.

Table 4. Selected Bond Distances (Å) and Angles (deg) for **4b**

Ru(1)–Ru(2)	2.4492(9)	Si(1)–C(1)	1.96(2)
Ru(1)–Si(1)	2.356(2)	Si(1)–C(2)	1.89(1)
Ru(2)–Si(1)	2.361(2)		
Ru(2)–Ru(1)–Si(1)	58.80(6)	Ru(1)–Ru(2)–Si(1)	58.64(5)
Ru(1)–Si(1)–Ru(2)	62.56(6)	C(1)–Si(1)–C(2)	101.9(9)

downfield shift of a ²⁹Si signal is typical of a bridging silylene ligand in a dinuclear complex containing an M–M interaction.⁵ The ²⁹Si signals of **4c** (Ph, Et) and **4a** (Ph, Ph) were also observed at lower magnetic field: at δ 291.7 and 265.0, respectively. With an increase in the number of phenyl groups on the bridging silicon, the ²⁹Si resonance of the mono(μ -silylene) complex shifted toward higher magnetic field. Such a trend was also found in bis(μ -silylene) complexes **3**.

Complex **1** reacts with only one molecule of vinylsilane, which contains an additional functional group besides an Si–H bond. Since the vinyl group and the Si–H bond occupied the vacant sites on the ruthenium centers effectively, coordination of the second molecule of vinylsilane would be suppressed. In the case of formation of the mono(μ -silylene) complex **4a**, which was obtained by the reaction of **1** with Ph₃SiH, coordination of the second silane was most likely suppressed by the steric hindrance of Ph₃SiH. The coordinated vinyl group, then, underwent hydrogenation by way of insertion into an Ru–H bond followed by reductive elimination.

Whereas the site-exchange process of the hydride ligands of bis(μ -silylene) complexes **3** was observed, it was revealed that mono(μ -silylene) complexes **4** were nonfluxional, at least on the NMR time scale, in the temperature range of 20–100 °C. Shapes of the hydride ligands were still sharp doublets, even at 100 °C. Different reactivities of mono(μ -silylene) complexes **4** in comparison to that of bis(μ -silylene) complexes **3** seemed to stem from such nonfluxionality.

An X-ray diffraction study was carried out using a red single crystal of **4b**. An ORTEP diagram of **4b** is depicted in Figure 4, and selected bond distances and angles are listed in Table 4. Bond lengths and angles are similar to those of the μ -diphenylsilylene complex **4a**. Two Cp* groups were located nearly parallel to each other; the angle between the centroids of the Cp* groups

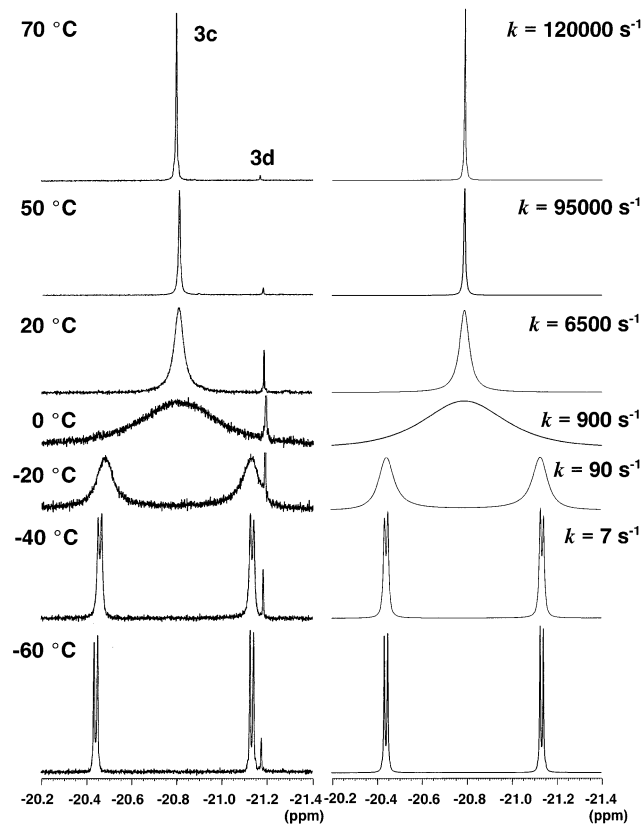


Figure 5. Variable-temperature ^1H NMR spectra of $\{\text{Cp}^*\text{Ru}(\mu\text{-H})_2(\mu\text{-SiMe}_2)(\mu\text{-SiPhMe})\}$ (**3c**) in $\text{THF-}d_8$ showing hydride signals (left) and results of the simulation (right). The small signal appearing at $\delta -21.16$ was assignable to the hydride signal of the bis(μ -silylene) complex $\{\text{Cp}^*\text{Ru}(\mu\text{-SiMe}_2)(\mu\text{-H})_2\}$ (**3d**).

and the Ru–Ru vector was ca. 3° . The Ru–Ru distance of 2.4492(9) Å corresponds to an Ru≡Ru triple bond. The Ru–Si lengths (average 2.359 Å) lie in the range of the reported value for a Ru–Si σ -bond and are similar to those of **4a** and bis(μ -silylene) complexes **3a,c**.

Fluxional Behavior of Bis(μ -silylene) Complex 3. (1) Site Exchange of the Hydride Ligands. As mentioned above, the site-exchange process of the hydride ligands took place in bis(μ -silylene) complexes **3**. Hydride signals of **3c** measured at various temperatures are depicted in Figure 5 together with simulated signals. At -60°C , the exchange process reached the slow-exchange limit and two sharp doublets of hydride ligands were found at $\delta -20.44$ and -21.13 . They began to exchange with an increase in temperature. The activation parameters of this process of **3c** were calculated on the basis of the Eyring plot using the exchange rate constant k obtained from the line-shape analysis; $\Delta H^\ddagger = 16.4 \pm 0.7 \text{ kcal mol}^{-1}$, $\Delta S^\ddagger = 15.5 \pm 2.6 \text{ cal mol}^{-1} \text{ K}^{-1}$. Those for **3b-syn** were also estimated at $\Delta H^\ddagger = 16.7 \pm 0.4 \text{ kcal mol}^{-1}$ and $\Delta S^\ddagger = 12.5 \pm 1.6 \text{ cal mol}^{-1} \text{ K}^{-1}$.

The X-ray diffraction study of **3c** showed that the silicon atoms were σ -bonded to two ruthenium atoms, and the small $^2J_{\text{Si-H}}$ value, 7–8 Hz, also showed that direct bonding interaction between Si and H was negligible. However, the existence of an intermediary species **A** having an Si–H bonding interaction is proposed in the site-exchange process (Scheme 3). Through rotation of the silyl group around the Ru–Si bond in the intermediate **A**, the hydride ligand migrates from

the back side to the front side of the Ru_2Si_2 plane. Oxidative addition of the Si–H bond of the intermediate **A** then affords the cis type intermediate **B**. Recently, we reported a similar site-exchange reaction via the formation of an intermediary μ -silyl complex during the site exchange of the hydride ligand of the μ -silylene μ -ethynyl complex $(\text{Cp}^*\text{Ru})_2(\mu\text{-SiMe}_2)(\mu\text{-CCH}_3)(\mu\text{-H})$,^{11b} and the existence of such a cis-type intermediate was implied by the reaction of a mixture of **3b-syn/anti** with PMe_3 (vide infra).

There are two possible pathways to account for the site-exchange process from the cis type intermediate **B**. In path A, reductive elimination between the other μ -silylene bridge and H^b to form the intermediate **A'** would take place. The hydride H^b then migrates to the back side of the Ru_2Si_2 plane by rotation of the μ -silyl group of **A'**, and as a result, H^a and H^b mutually exchange the coordination site without change in the orientation of the substituents on the bridging silicon atoms. Path B includes reductive coupling between H^a and H^b to form the η^2 -hydrogen intermediate **C**. Rotation of the $\eta^2\text{-H}_2$ ligand on the ruthenium center would result in site exchange between H^a and H^b .

Complex **3c** has both $\mu\text{-SiPhMe}$ and $\mu\text{-SiMe}_2$ bridges. It is likely that the energy barrier to make an Si–H bond is different. Lichtenberger et al. have shown that electron-withdrawing substituents on the silicon promote the oxidative addition of an Si–H bond due to lowering the energy level of $\sigma^*(\text{Si-H})$.²⁰ Therefore, it seems to be preferable to form a $\mu\text{-HSiMe}_2$ group rather than to form a $\mu\text{-HSiPhMe}$ group during the site-exchange reaction.

There were, however, no distinct differences between the activation parameters of **3c** and **3b-syn**. There were two possible explanations for this result. The first explanation is that formation of the $\mu\text{-HSiPhMe}$ group was involved in the rate-determining step in both processes of **3c** and **3b-syn**. Since formation and rotation of the two silyl ligands were required for the hydride site exchange by path A in Scheme 3, the step of the formation of $\mu\text{-HSiPhMe}$, which was considered to be higher than that of $\mu\text{-HSiMe}_2$, would be included in both cases. The second explanation is that the step of formation and cleavage of an intermediary Si–H bond is not involved in the rate-determining step of the fluxional process. The kinetic parameters for **3c** and **3b** are almost the same, regardless of the substituents on the silicon atoms. Therefore, the site-exchange process of the hydrides most likely proceeds via the intermediary η^2 -hydrogen complex **C** (path B in Scheme 3).

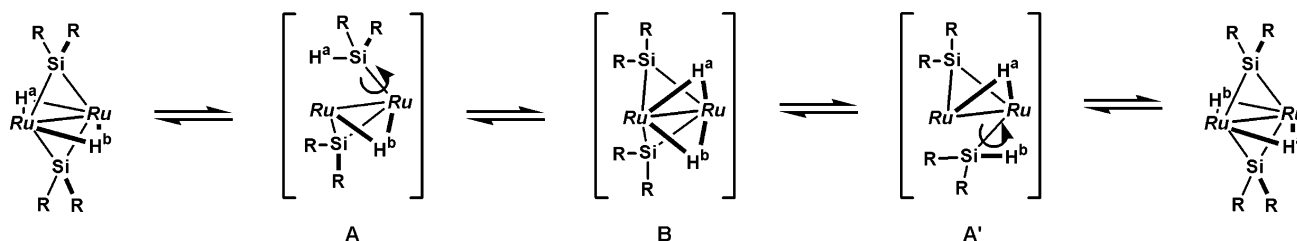
It is difficult to conclude whether path A or path B is plausible at this stage, because both complexes, **3c** and **3b**, have the $\mu\text{-SiPhMe}$ bridge. We are now trying to synthesize another type of mixed-bridge bis(μ -silylene) complex not containing a $\mu\text{-SiPhMe}$ bridge, and information about the mechanism would be obtained in detail by VT-NMR studies on these complexes.

The ^{29}Si signals of bis(μ -silylene) complexes **3** were observed around $\delta 110$ (**3a**, $\delta 109.8$; **3b-syn/anti**, $\delta 108.2, 107.7$; **3c**, $\delta 112.3, 107.9$), which were consider-

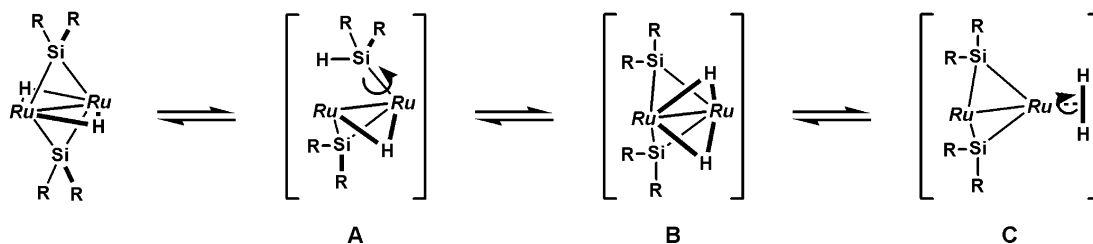
(20) (a) Lichtenberger, D. L.; Rai-Chaudhuri, A. *J. Am. Chem. Soc.* **1989**, *111*, 3583–3591. (b) Lichtenberger, D. L.; Rai-Chaudhuri, A. *Inorg. Chem.* **1990**, *29*, 975–981. (c) Lichtenberger, D. L.; Rai-Chaudhuri, A. *Organometallics* **1990**, *9*, 1686–1690. (d) Lichtenberger, D. L.; Rai-Chaudhuri, A. *J. Am. Chem. Soc.* **1990**, *112*, 2492–2497.

Scheme 3^a

(path A)



(path B)

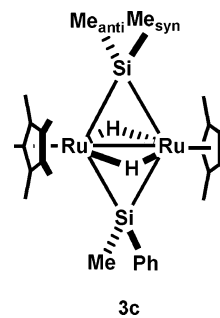
Ru = (C₅Me₅)Ru^a Ru = (C₅Me₅)Ru.

ably higher than the reported values for the bridging silylene atoms. They were much different from those of mono(μ -silylene) complexes (**4a**, δ 265.0; **4b**, δ 310.8; **4c**, δ 291.7), despite the fact that they have similar structures around the bridging silicon atom. The reason the ²⁹Si signals of **3** appeared at higher region is most likely due to the fluxional process in which the intermediary Si–H bonds were held. They were rather close to those for bis(μ -silyl) complexes having 2e–3c Ru–H–Si interactions. The ²⁹Si signals of {Cp*₂Ru(μ - η^2 -HSiPh₂)}₂(μ -H)(H) (**2a**) and {Cp*₂Ru(μ - η^2 -HSiPhMe)}₂(μ -H)(H) (**2b-syn**) were observed at δ 95.1 and 101.9, respectively. Although $J_{\text{Si-H}}$ values of these bis(μ -silylene) complexes **3** were determined to be less than 10 Hz from the observed satellite signals in the ¹H NMR spectra, the bridging silicon ligand of **3** seems to have some contribution of a μ -silyl ligand in solution. Downfield shifts of the ²⁹Si signals of mono(μ -silylene) complexes **4** were thus most likely attributed to a lack of Si–H interaction. This is the significantly different point between complexes **3** and **4** in their properties.

(2) Rotation of the Bridging Silicon Atom. The site-exchange reaction of the methyl groups on the μ -SiMe₂ bridge also took place in **3c** (Chart 1) at higher temperature (Figure 6). Line-shape analysis of this fluxional process revealed that the site-exchange process of the methyl groups took place independently of that of the hydride ligands ($\Delta H^\ddagger = 16.5 \pm 0.7$ kcal mol⁻¹, $\Delta S^\ddagger = -7.8 \pm 2.1$ cal mol⁻¹ K⁻¹).

There were two possible pathways of the site exchange of the methyl groups between the syn methyl group and that anti to the phenyl group. Path A involves isomerization of the μ -SiMe₂ (or μ -SiPhMe) ligand to a terminally bonded silylene ligand followed by rotation around an Ru=Si bond. Path B involves a 1,2-shift of the intermediary μ -silyl ligand. Although rotation of the

Chart 1

**3c**

Ru=Si bond is often proposed for some isomerization of μ -silylene complexes,^{8j,21} it would bring about a larger positive ΔS^\ddagger value due to steric repulsion between two Cp* groups. The ΔS^\ddagger value of -8 cal mol⁻¹ K⁻¹ is very similar to the site-exchange process of the methyl groups of (Cp*₂Ru)₂(μ -SiMe₂)(μ -CCH₃)(μ -H) ($\Delta H^\ddagger = 12.5 \pm 0.1$ kcal mol⁻¹, $\Delta S^\ddagger = -7.7 \pm 0.4$ cal mol⁻¹ K⁻¹)^{11b} by way of a 1,2-shift of the intermediary silyl group (path B in Scheme 4). Migration of the silyl group between the two ruthenium nuclei proceeded with retention of the stereochemistry at the silicon atom. Oxidative addition of the Si–H bond at Ru² resulted in the isomerization between syn and anti forms (inversion of the μ -silylene ligand). Migration of the PR₃ group on the diruthenium skeleton with retention at the phosphorus atom was reported in our preceding paper, and the transition state of the dynamic process was proposed by the aid of DFT calculations.²² Girolami et al. have also reported the 1,2-shift of a silyl group on the diruthenium complex (Cp*₂Ru)₂(μ -CH₂)(SiMe₃)(Cl). In this process, the activa-

(21) Kummer, D.; Furrer, J. Z. Naturforsch., B **1971**, 26B, 162–163.(22) Ohki, Y.; Suzuki, H. Angew. Chem., Int. Ed. **2002**, 41, 2994–2997.

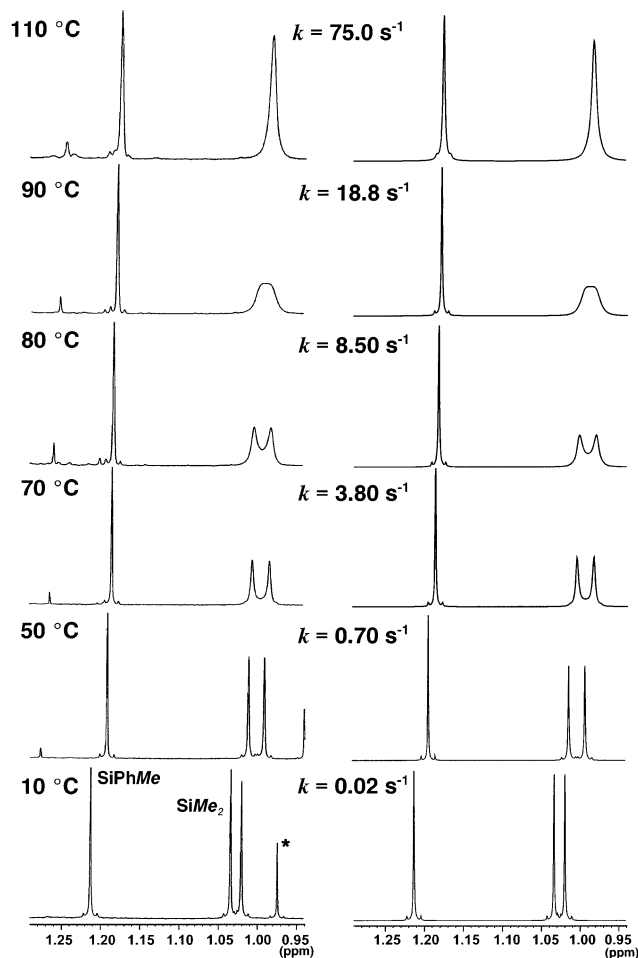


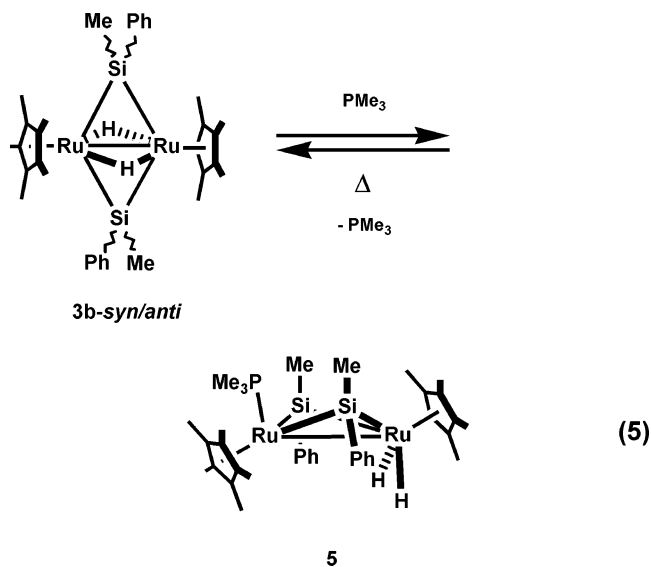
Figure 6. Variable-temperature ^1H NMR spectra of $\{\text{Cp}^*\text{Ru}(\mu\text{-H})_2(\mu\text{-SiMe}_2)(\mu\text{-SiPhMe})\}$ (**3c**) in toluene- d_8 showing methyl signals (left) and results of simulation (right). The small signal marked with an asterisk appearing at δ 0.97 at 10 $^\circ\text{C}$ was assignable to the methyl signal of the bis(μ -silylene) complex $\{\text{Cp}^*\text{Ru}(\mu\text{-SiMe}_2)(\mu\text{-H})_2\}$ (**3d**).

tion parameters, ΔH^\ddagger and ΔS^\ddagger , were estimated at 9.0 ± 0.2 kcal mol $^{-1}$ and 0.5 ± 0.8 cal mol $^{-1}$ K $^{-1}$, respectively.²³

Although isomerization between **3b-syn** and **3b-anti** was not observed in the VT-NMR study, which was most likely due to the small difference in ΔS^\ddagger , isomerization of **3b-anti** to the syn form was confirmed in the reaction of a mixture of **3b-syn/anti** with PMe_3 . This isomerization is also considered to proceed via the 1,2-shift of an intermediary μ -silyl group.

Reaction of a Mixture of the Bis(μ -phenylmethylsilylene) Complex **3b with PMe_3 : A Trapped Complex of the *cis*-Bis(μ -silylene) Intermediate by PMe_3 .** While bis(μ -diphenylsilylene) complex **3a** did not react with PMe_3 irrespective of reaction temperature, treatment of a mixture of the two diastereomers **3b-syn/anti** with a small excess amount of PMe_3 afforded bis(μ -silylene) complex $\{\text{Cp}^*\text{Ru}(\mu\text{-SiPhMe})_2(\text{PMe}_3)(\text{H})_2\}$ (**5**) as the sole product (eq 5). Notably, only syn-**5** was obtained during the reaction, although the reaction was carried out using a mixture of syn and anti isomers. The

PMe_3 coordinated in **5** was readily liberated upon heating, and a thermodynamic mixture of two diastereomers of **3b** (syn:anti = 55:45) was recovered. This showed an occurrence of geometrical change from syn to anti with respect to the silylene bridges, and this geometrical change is probably a result of rotation of the silylene group around the Ru–Si bond. The bis(μ -silylene) complex **5** was fully characterized on the basis of ^1H , ^{13}C , ^{29}Si , and ^{31}P NMR and IR spectra as well as elemental analysis.



In the ^1H NMR spectra measured at 23 $^\circ\text{C}$, two singlets with the same intensity assignable to the Cp^* groups were observed at δ 1.20 and 1.84. The former was observed as a doublet with a coupling constant of $J_{\text{P-H}} = 0.7$ Hz. This strongly indicates that the PMe_3 ligand is coordinated to one of the two ruthenium centers as a terminal ligand. In contrast, the hydride signal was observed as a singlet at δ -13.06 with an intensity ratio of 2H. This indicates terminal coordination of these hydride ligands to the ruthenium atom which has no bonding interaction with the phosphine ligand. A sharp absorption attributable to $\nu(\text{Ru-H})$ was observed at 2036 cm^{-1} in the IR spectrum of **5**.

The two methyl groups on the bridging silicon atoms were observed to be equivalent. This indicates that **5** adopts a syn form with respect to the orientation of the two μ -SiPhMe groups. The ^{29}Si signal of **5** was observed at δ 205.2 as a doublet peak with a coupling constant of $J_{\text{Si-P}} = 20.5$ Hz.

At -40 $^\circ\text{C}$, two signals assignable to the methyl protons of PMe_3 were observed at δ 1.35 (d, 6H, $J_{\text{P-H}} = 7.9$ Hz) and 1.11 (d, 3H, $J_{\text{P-H}} = 7.9$ Hz), respectively. These signals coalesced into one signal at 60 $^\circ\text{C}$. Free rotation around the Ru–P bond was interrupted, most likely due to steric repulsion between two Si–Me groups and one P–Me group. An X-ray diffraction study revealed that one P–C bond lay between two Si–Me groups, which was clearly shown in a space-filling model of the $\text{Ru}_2\text{Si}_2\text{P}$ moiety (Figure 8).

X-ray diffraction studies were carried out using a yellow single crystal of **5** obtained from cold pentane solution. An ORTEP diagram of **5** is depicted in Figure 7, and selected bond distances and angles are listed in

(23) (a) Lin, W.; Wilson, S. R.; Girolami, G. S. *J. Am. Chem. Soc.* **1993**, *115*, 3022–3023. (b) Lin, W.; Wilson, S. R.; Girolami, G. S. *Organometallics* **1991**, *13*, 2309–2319.

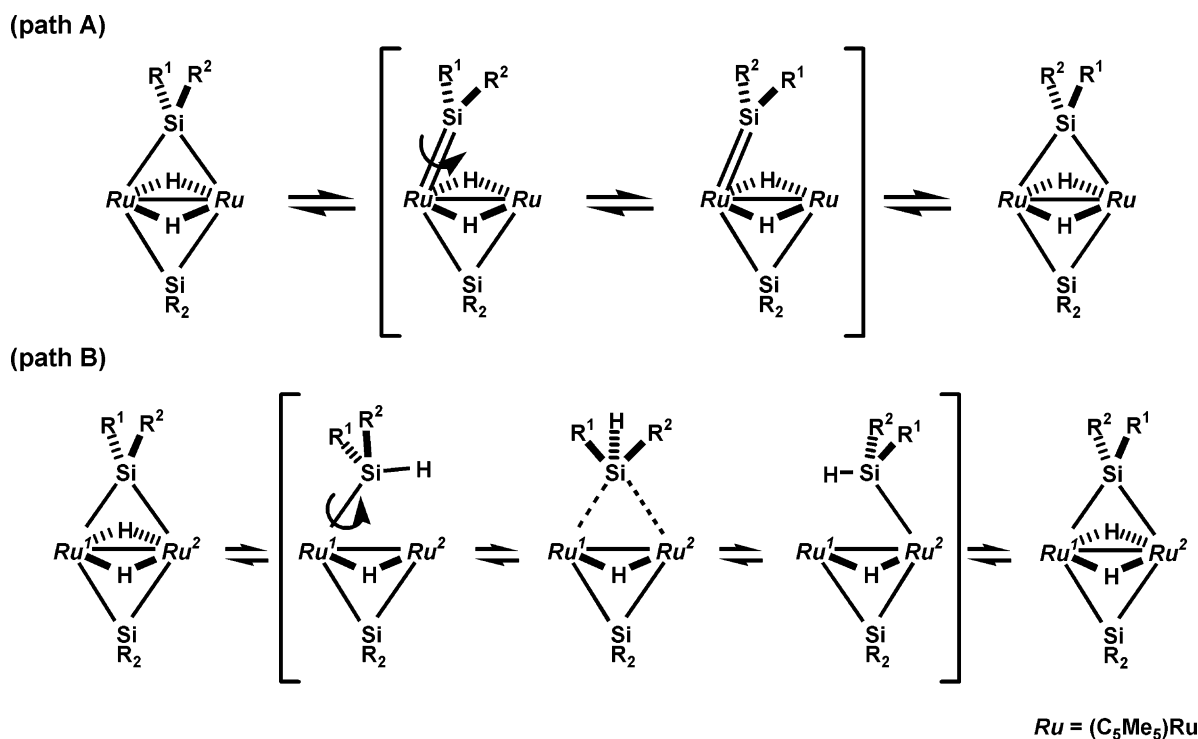
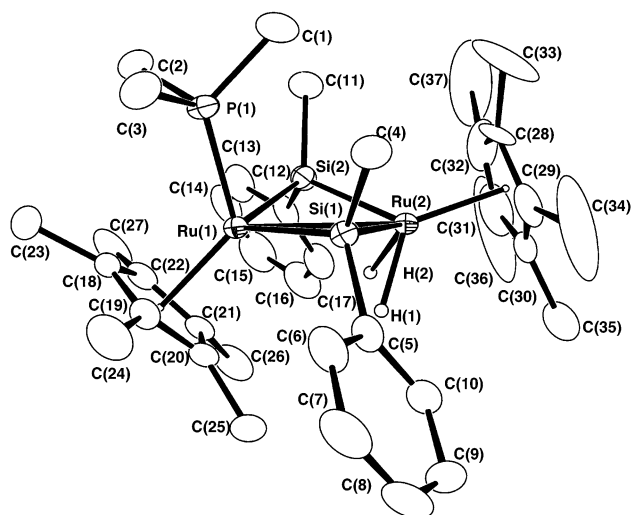
Scheme 4^a^a $Ru = (C_5Me_5)Ru$.

Figure 7. Molecular structure of $\{Cp^*Ru(\mu-SiPhMe)\}_2-(PMe_3)(H)_2$ (**5**), with thermal ellipsoids at the 30% probability level.

Table 5. Location of the terminal hydride ligands was determined during Fourier synthesis and refined isotropically. The Ru(1)–Ru(2) distance (3.0159(18) Å) indicated there was a single bonding interaction between two ruthenium atoms. Each metal center satisfied the EAN rule from consideration of a single Ru–Ru bond.

It was clearly seen in Figure 7 that two hydride ligands and two silylene ligands were both attached to Ru(2) in a cis fashion. Bridging SiPhMe groups in **5** are mutually cis with respect to the Ru–Ru vector, and **5** is likely formed as a result of capture of the intermediary *cis*-silylene species proposed in the site exchange of the hydride ligands.

Despite the steric repulsion between the P–Me and the Si–Me groups implied on the basis of the VT-NMR study of **5**, apparent elongation of the Ru(1)–P(1) bond was not observed. The steric repulsion was clearly reflected in the bond angles. The value of 95.5° for the C–Si–C angle was considerably small for an sp³ silicon atom, and the Ru(1)–P(1)–C(1) angle is larger than Ru(1)–P(1)–C(2) and Ru(1)–P(1)–C(3) by ca. 10°. The Ru(1)–P(1) length lies in the normal range of the reported Ru–P bond lengths in the $[Cp^*Ru(PMe_3)]_2$ unit (2.258–2.374 Å).²⁴ The Ru(1)–P(1) length of 2.260(2) Å is almost the same as that observed in $\{Cp^*Ru(\mu-H)\}_2-(PMe_3)$ (2.278(5) Å), which was obtained by the reaction of **1** with PMe_3 .²² All of the Ru–Si lengths also lie in the normal range for Ru–Si σ-bonds.

Either **3b-syn** or **3b-anti** reacts with PMe_3 to afford the syn isomer of **5**, whose methyl groups on the bridging silicon atom occupy the axial positions. Thus, during this reaction, the syn/anti isomerization took place simultaneously with the cis/trans isomerization of the bis(*μ*-silylene) complex. As mentioned above, the syn to anti ratio of **3b** did not change at least up to 70 °C. This means that isomerization from **3b-anti** to **3b-syn** was slow or did not proceed at ambient temper-

(24) For example: (a) Straus, D. A.; Tilley, T. D.; Reingold, A. L.; Geib, S. J. *J. Am. Chem. Soc.* **1987**, *109*, 5872–5873. (b) Lehmkuhl, H.; Schwickardi, R.; Kruger, C.; Raabe, G. *Z. Anorg. Allg. Chem.* **1990**, *581*, 41–47. (c) Grumbine, S. D.; Chadha, R. K.; Tilley, T. D. *J. Am. Chem. Soc.* **1992**, *114*, 1518–1520. (d) Schenk, W. A.; Urban, P.; Dombrowski, E. *Chem. Ber.* **1993**, *126*, 679–684. (e) Grumbine, S. K.; Tilley, T. D.; Arnold, F. P.; Rheingold, A. L. *J. Am. Chem. Soc.* **1994**, *116*, 5495–5496. (f) Dombrowski, E.; Schenk, W. A. *Angew. Chem., Int. Ed. Engl.* **1995**, *34*, 1008–1009. (g) Mitchell, G. P.; Tilley, T. D. *J. Am. Chem. Soc.* **1997**, *119*, 11236–11243. (h) Grumbine, S. K.; Mitchell, G. P.; Straus, D. A.; Tilley, T. D.; Rheingold, A. L. *Organometallics* **1998**, *17*, 5607–5619. (i) Smith, D. C., Jr.; Haar, C. M.; Luo, L.; Li, C.; Cucullu, M. E.; Mahler, C. H.; Nolan, S. P.; Marshall, W. J.; Jones, N. L.; Fagan, P. J. *Organometallics* **1999**, *18*, 2357–2361. (j) Kawano, Y.; Shimoi, M. *Chem. Lett.* **1999**, 489–490.

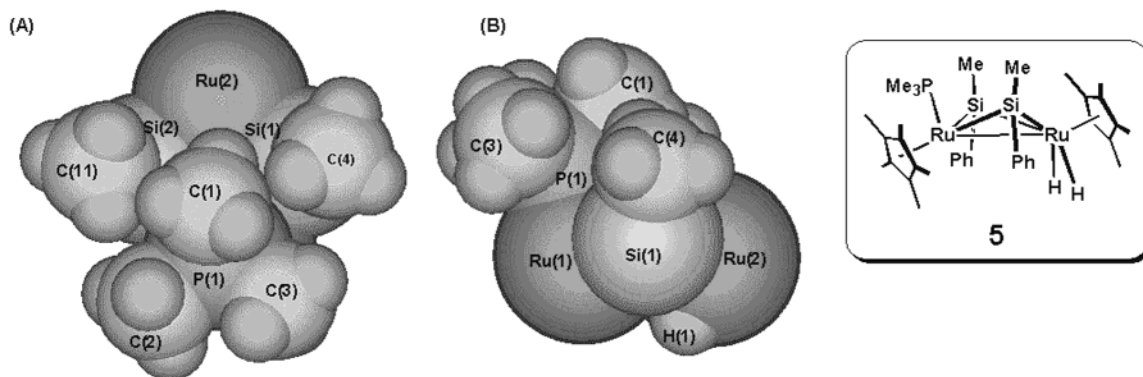


Figure 8. Space-filling model of the $\text{Ru}_2\text{Si}_2\text{P}$ moiety of complex **5**: (A) top view; (B) side view.

Table 5. Selected Bond Distances (Å) and Angles (deg) for 5

Ru(1)–Ru(2)	3.0159(18)	Ru(1)–P(1)	2.260(2)
Ru(1)–Si(1)	2.358(2)	Ru(1)–Si(2)	2.365(3)
Ru(2)–Si(1)	2.391(3)	Ru(2)–Si(2)	2.382(3)
Ru(2)–H(1)	1.66(7)	Ru(2)–H(2)	1.75(8)
P(1)–C(1)	1.832(10)	P(1)–C(2)	1.841(9)
P(1)–C(3)	1.824(10)	Si(1)–C(4)	1.926(9)
Si(1)–C(5)	1.924(8)	Si(2)–C(11)	1.917(9)
Si(2)–C(12)	1.912(9)		
Si(1)–Ru(1)–Si(2)	98.27(8)	Si(1)–Ru(2)–Si(2)	96.90(8)
H(1)–Ru(2)–H(2)	62(4)	Ru(1)–P(1)–C(1)	124.3(4)
Ru(1)–P(1)–C(2)	113.9(4)	Ru(1)–P(1)–C(3)	115.9(4)
Ru(1)–Si(1)–Ru(2)	78.85(7)	Ru(1)–Si(2)–Ru(2)	78.90(7)
C(4)–Si(1)–C(5)	94.1(4)	C(11)–Si(2)–C(12)	96.8(4)

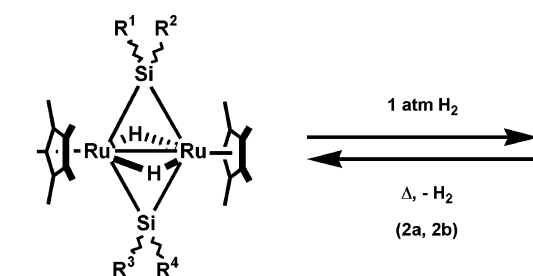
ature. Therefore, trimethylphosphine seemed to cause the isomerization from the anti to the syn isomer.

In contrast to the syn/anti isomerization, the site exchange of the hydride ligands of **3b** took place at room temperature at a considerable rate. This indicates that the *cis*-bis(μ -silylene) intermediates would be generated during the reaction independently of PMe_3 (step A in Scheme 5). Thus, the syn/anti isomerization involved in step B in Scheme 5 should be accelerated by the presence of PMe_3 . Interaction of PMe_3 with **3b** would afford a **34e** intermediate, which was coordinatively saturated. In this intermediate, rotation of the μ -silylene bridge would be promoted due to the steric repulsion.

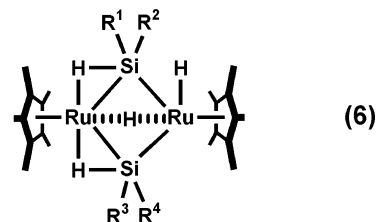
The reaction of **3b** with PMe_3 showed both *cis*/*trans* and syn/anti isomerization occurring in the bis(μ -silylene) complex, and this result is quite consistent with the VT-NMR studies. Formation of the *cis*-bis(μ -silylene) intermediate is the key step of the unique reactivity of the bis(μ -silylene) complex **3**. The reaction of **3a** with acetylene afforded a μ -disilaruthenacyclopentene complex, which also adopted a *cis* form.^{11a} Complex **3** also reacts with H_2 and CO, as mentioned below. These reactions were thought to proceed via formation of the *cis*-bis(μ -silylene) intermediate.

Reaction of Bis(μ -silylene) Complex 3 with Dihydrogen: Formation of Bis(μ -silyl) Complex 2. Treatment of bis(μ -silylene) complexes **3a–c** with 1 atm of dihydrogen at ambient temperature quantitatively afforded the bis(μ -silyl) complexes $\{\text{Cp}^*\text{Ru}(\mu\text{-}\eta^2\text{-HSiR}^1\text{R}^2)\}\text{-}\{\text{Cp}^*\text{Ru}(\mu\text{-}\eta^2\text{-HSiR}^3\text{R}^4)\}(\mu\text{-H})(\text{H})$ (**2a**, $\text{R}^1 = \text{R}^2 = \text{R}^3 = \text{R}^4 = \text{Ph}$; **2b-syn** and **2b-anti**, $\text{R}^1 = \text{R}^3 = \text{Ph}$, $\text{R}^2 = \text{R}^4 = \text{Me}$; **2c**, $\text{R}^1 = \text{R}^2 = \text{R}^3 = \text{Me}$, $\text{R}^4 = \text{Ph}$), respectively (eq 6). The rate of hydrogenation of **3** significantly depended on the substituents on the bridging silicon atoms. While completion of the reaction of the bis(μ -diphenylsilylene)

complex **3a** with 1 atm of H_2 took 48 h at 25 °C, formation of **2c** was accomplished within 2 h under 1 atm of H_2 atmosphere.



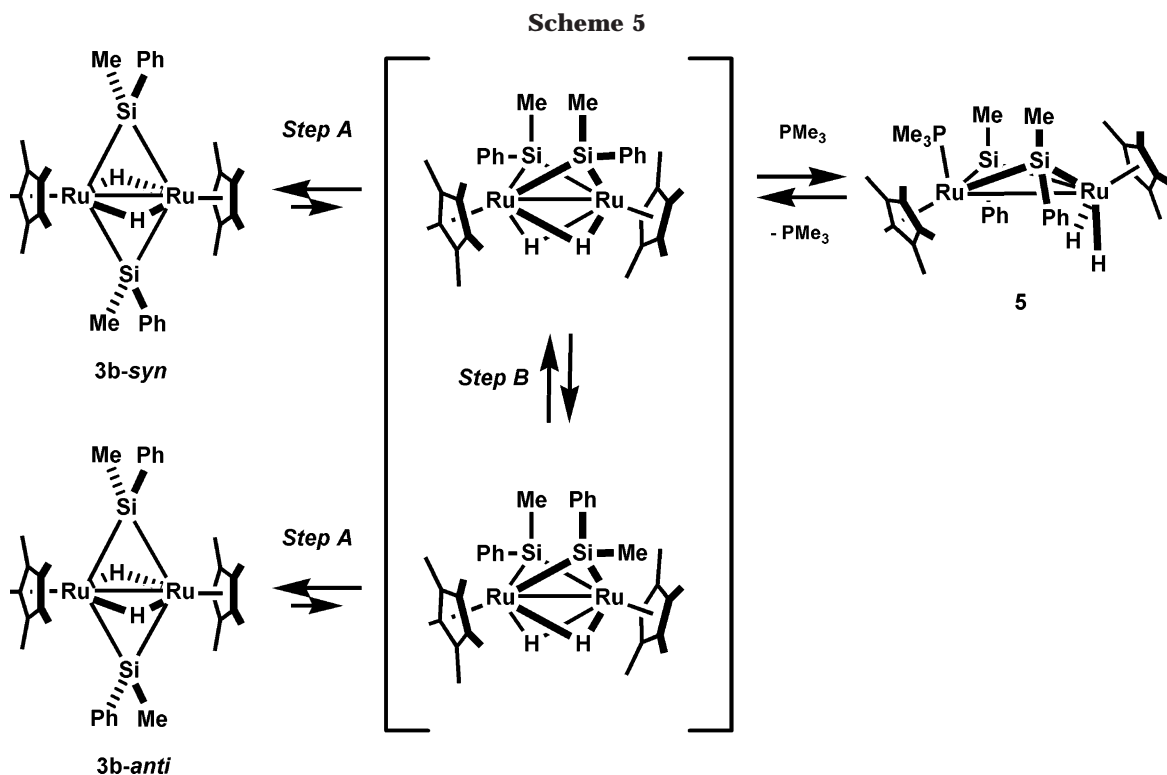
3a; $\text{R}^1 = \text{R}^2 = \text{R}^3 = \text{R}^4 = \text{Ph}$
3b; $\text{R}^1 = \text{R}^3 = \text{Ph}$, $\text{R}^2 = \text{R}^4 = \text{Me}$
3c; $\text{R}^1 = \text{R}^2 = \text{R}^3 = \text{Me}$, $\text{R}^4 = \text{Ph}$



2a; $\text{R}^1 = \text{R}^2 = \text{R}^3 = \text{R}^4 = \text{Ph}$
2b; $\text{R}^1 = \text{R}^3 = \text{Ph}$, $\text{R}^2 = \text{R}^4 = \text{Me}$
2c; $\text{R}^1 = \text{R}^2 = \text{R}^3 = \text{Me}$, $\text{R}^4 = \text{Ph}$

The reverse reaction of eq 6, oxidative addition of the $\eta^2\text{-Si-H}$ bonds of the bis(μ -silyl) complex **2**, proceeds more readily in **2a** than in **2b-syn/anti**. Complex **2c**, which has one phenyl group on the bridging silicon atoms, did not undergo oxidative addition of the $\eta^2\text{-Si-H}$ bonds upon heating in solution. On the other hand, thermolysis of **2c** resulted in decomposition to yield a messy mixture. Complex **3c** also gradually decomposed even at -20 °C to yield a complex mixture, including the diruthenium tetrahydride complex **1**; the half-life of **3c** is about 1 month at -20 °C under an argon atmosphere. Thus, thermal stability of the Ru–Si bond in **3** is affected by the substituents on the bridging silicon atoms as well as the rate of hydrogenation of **3**.

It is known that an electron-withdrawing phenyl group lowers the energy level of the $\sigma^*(\text{Si-H})$. Thus, as the number of phenyl groups is increased, oxidative addition of the Si–H bond proceeds readily, and the equilibrium is inclined toward the bis(μ -silylene) complex. This is fully consistent with the photoelectron



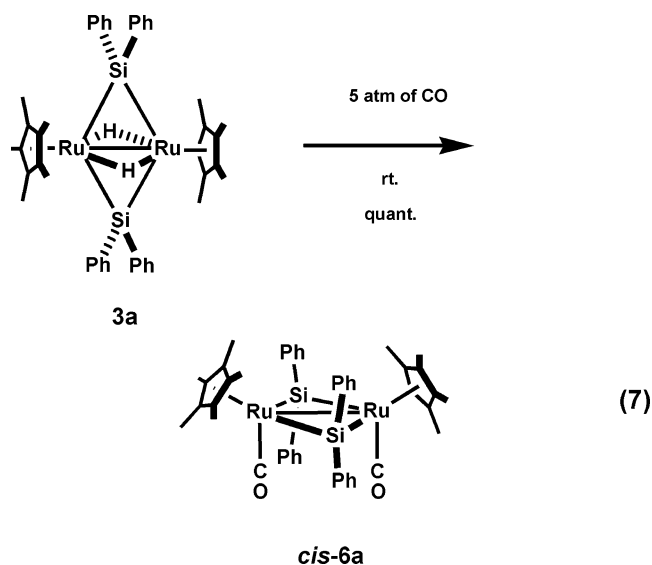
studies of silane complexes having 2e–3c M–H–Si interactions performed by Lichtenberger et al.²⁰

Complexes **2a,e** have been alternatively synthesized by the reaction of **1** with Ph₂SiH₂ and Et₂SiH₂, respectively.^{7a} A diastereomeric mixture of the μ -phenylmethylsilyl complex {Cp*Ru(μ -HSiPhMe)}₂(μ -H)(H) (**2b-syn/anti**) was also obtained by the reaction of **1** with PhMeSiH₂.²⁵ Whereas **3b-syn** and **3b-anti** could not be separated by the use of column chromatography, **2b-syn** and **2b-anti** could be separated from each other. Orientation of the substituents on the bridging silyl groups of **2b-syn** and **2b-anti** could be determined by the use of ¹H NMR.

The mono(μ -silylene) complex **4** has both bridging silylene and hydride ligands, and its structural parameters around the silicon atom were quite similar to those of **3**. Thus, formation of a mono(μ -silyl) or mono(μ -silane) complex would be anticipated by the reaction with dihydrogen. However, the reaction of **4** with dihydrogen proceeded in a way considerably different from that of **3**. While the bis(μ -silylene) complex **3** readily reacted with dihydrogen at ambient temperature, the mono(μ -silylene) complex **4** did not react with dihydrogen without heating. Complex **4** only reacted under more severe conditions; it required 100 °C and 7 atm of H₂. Neither a mono(μ -silyl) nor a mono(μ -silane) complex was obtained by the reaction. Instead, a mixture of tetrahydride complex **1** and its thermolysis products was obtained.²⁶ Formation of **1** indicates liberation of the bridging diphenylsilylene ligand, but the fate of the bridging silylene moiety has not yet been clarified.

Reaction of Bis(μ -silylene) Complex **3 with Carbon Monoxide.** The bis(μ -silylene) complex **3** was a 32-

electron complex. Thus, coordinative addition of the 2e donor to **3** was anticipated. Since trimethylphosphine was bulky, only one molecule was incorporated into **3b**. Furthermore, complex **3a** did not react with PMe₃ because of steric repulsion between the four phenyl groups and phosphine. In contrast to this, when using carbon monoxide, which is a less bulky 2e donor, the bis(μ -silylene) complex **3a** reacts with 2 molar equiv of CO. The reaction of **3a** with carbon monoxide smoothly proceeds at room temperature to form the dicarbonyl complex {Cp*Ru(μ -SiPh₂)(CO)}₂ (**cis-6a**) (eq 7). The two



CO groups were coordinated to the Ru₂Si₂ plane in a cis fashion. In a previous paper,^{7a} we proposed the wrong geometry for the dicarbonyl complex formed in the reaction of **3a** with carbon monoxide. Here we correct the structure of **6a** for the mistakes in the geometry of two carbonyl groups. The cis geometry of **6a** was revealed by detailed spectroscopic studies as well

(25) Takao, T.; Suzuki, H. Unpublished results (see the Supporting Information).

(26) Suzuki, H.; Omori, H.; Ito, Y. Unpublished results. Thermolysis of a diruthenium tetrahydride complex in toluene at 100 °C afforded a mixture of polyhydride clusters of {Cp*Ru(μ -H)}₃(μ_3 -H)₂ and (Cp*Ru)₄(H)₆ in the ratio ca. 95:5.

as preliminary X-ray diffraction studies. Complex **6a** was fully characterized on the basis of ^1H , ^{13}C , and ^{29}Si NMR, IR, and FD-MS spectra as well as elemental analysis.

A yellow single crystal of *cis*-**6a** was obtained from cold toluene solution, but the quality was not good enough for X-ray diffraction studies. However, *cis* coordination of the two terminal CO ligands with respect to the Ru_2Si_2 plane was unquestionably confirmed (see Figure S-1 in the Supporting Information).

The *cis* coordination of the CO ligands was also confirmed by means of IR and ^{13}C NMR spectroscopy. In the IR spectrum of *cis*-**6a**, a band assignable to the symmetric stretching mode of the carbonyl ligands was observed at 1955 cm^{-1} , and that of the asymmetric mode was observed at 1922 cm^{-1} as a shoulder peak. The intensity ratio of $\nu_{\text{sym}}/\nu_{\text{asym}}$ was larger than 1, which indicates *cis* coordination of the two CO ligands with respect to the Ru_2Si_2 plane. Observation of two sets of ^{13}C signals of the phenyl groups in the ^{13}C NMR spectra also indicates *cis* coordination of the carbonyl ligands.

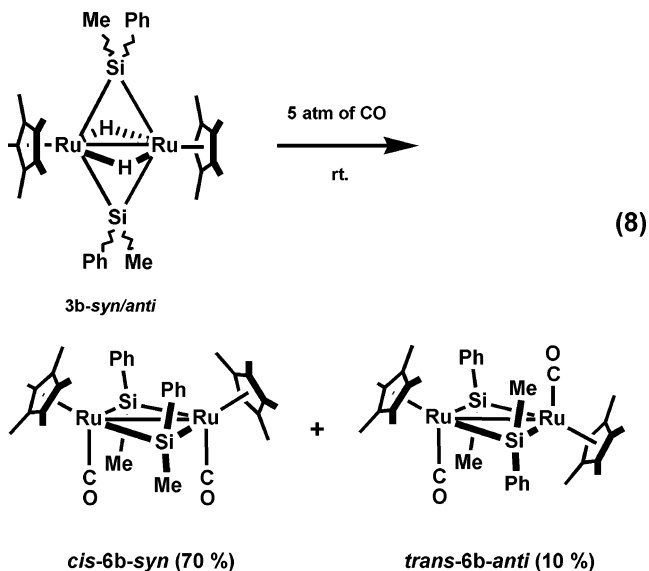
In the ^{29}Si NMR spectra of *cis*-**6a**, the resonance of the bridging silylene ligand was observed at δ 211.4. The remarkable downfield shift compared to that of **3a** (δ 109.8) can most likely be attributed to lack of interaction between Si and H.

Ogino et al. reported thermal and photochemical isomerization between *cis*- and *trans*- μ -silylene complexes $\text{Cp}_2\text{Fe}_2(\text{CO})_2(\mu\text{-CO})\{\mu\text{-SiMe}(\text{SiMe}_3)\}$, in which cleavage of an Fe–Fe bond was involved.²⁷ In the case of **6a**, however, formation of the *trans* isomer of **6a** was not observed during the reaction. The complex *cis*-**6a** was thermally robust, and isomerization to the *trans* isomer did not take place, at least at $150\text{ }^\circ\text{C}$. In contrast to the mono(μ -silylene) mono(μ -carbonyl) diiron complex, cleavage of the Ru–Ru bond followed by rotation around the Ru–Si bond would not take place, since the two ruthenium atoms of *cis*-**6a** were strongly bound by the two bridging silicon atoms.

Although no intermediate was observed during the reaction, the complex *cis*-**6a** would be formed via the intermediary *cis*-bis(μ -silylene) complex in analogy to the formation path of **5**, and the hydride ligands were substituted by the second CO molecule.

The diastereomeric mixture **3b-syn/anti** also reacted with carbon monoxide to give *cis*-**6b-syn** and *trans*-**6b-anti** (eq 8), but the reaction was much more complicated; in the IR spectra of the obtained mixture, several bands arising from the byproducts containing a bridging carbonyl ligand were observed around $1750\text{--}1800\text{ cm}^{-1}$. The spectra indicate that the mono(μ -silylene) complex $\{\text{Cp}^*\text{Ru}(\text{CO})\}_2(\mu\text{-SiPhMe})(\mu\text{-CO})$ and the diruthenium tetracarbonyl complex $\{\text{Cp}^*\text{Ru}(\text{CO})\}_2(\mu\text{-CO})_2$ (**7**)²⁸ were formed in addition to *cis*-**6b-syn** and

trans-**6b-anti**. Formation of **7** was confirmed on the basis of the ^1H NMR and IR spectra of the mixture.



Only two isomers, *cis*-**6b-syn** and *trans*-**6b-anti**, were isolated by the use of column chromatography followed by recrystallization. The major isomer was *cis*-**6b-syn**, which was obtained in 70% yield. The ^1H and ^{13}C NMR spectra and IR spectrum of *cis*-**6b-syn** indicated a *cis* geometry of the two carbonyl groups with respect to the Ru_2Si_2 plane, as in *cis*-**6a**, and the orientation of the two bridging silicon atom was revealed as a *syn* form similar to that of **5**.

In the ^1H NMR spectra of *cis*-**6b-syn**, one singlet assignable to the methyl group on the bridging silicon was observed at δ 1.55. In the IR spectra of *cis*-**6b-syn**, ν_{sym} and ν_{asym} were observed at 1932 and 1903 cm^{-1} , respectively. The *cis* orientation of the two carbonyl groups was confirmed by the fact that the intensity ratio of $\nu_{\text{sym}}/\nu_{\text{asym}}$ was larger than 1.

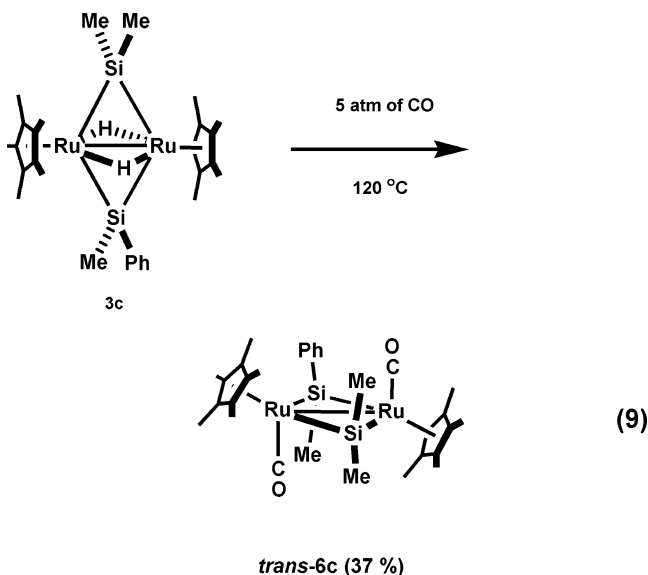
In contrast to *cis*-**6b-syn**, *trans*-**6b-anti** adopted a *trans* form with respect to the Ru_2Si_2 plane. In the IR spectrum of *trans*-**6b-anti**, only absorption assignable to ν_{asym} was observed at 1899 cm^{-1} . In addition to this, only one signal assignable to the methyl groups on the bridging silicon atoms was observed at δ 1.41. These facts imply that two carbonyl groups coordinate to the Ru_2Si_2 plane in a *trans* fashion, and the orientation of the two silicon atoms is an *anti* form.

Formation of the *trans* isomer was also observed in the reaction of **3c** with CO. The *trans*-dicarbonyl complex $\{\text{Cp}^*\text{Ru}(\text{CO})\}_2(\mu\text{-SiPhMe})(\mu\text{-SiMe}_2)$ (*trans*-**6c**) was isolated in 37% yield among many products by the use of column chromatography (eq 9). In the ^1H NMR spectrum of *trans*-**6c**, two ^1H signals of the Cp^* group were observed at δ 1.61 and 1.74 with the same intensity. This unquestionably indicates the *trans* geometry of **6c**. *Trans* geometry was also confirmed by the IR spectrum, showing a strong absorption assignable to the asymmetric mode of $\nu(\text{CO})$ at 1903 cm^{-1} .

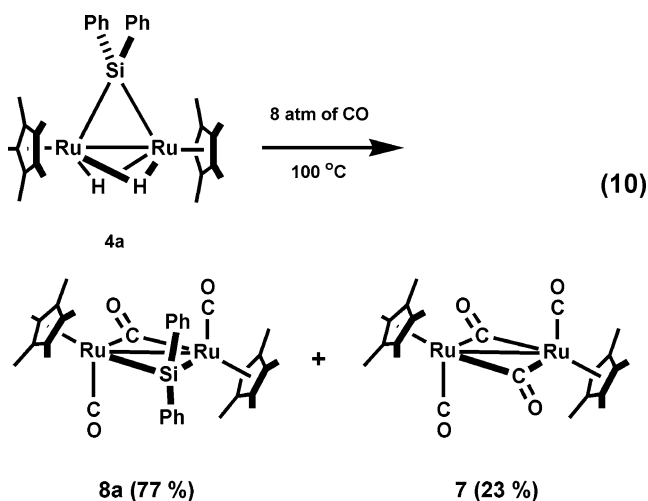
Reaction of Mono(μ -silylene) Complexes **4 with Carbon Monoxide.** While the reaction of the mono(μ -silylene) complex **4** with dihydrogen resulted in liberation of the bridging silicon atom, a μ -carbonyl complex containing a bridging silylene ligand was obtained in the reaction of **4** with CO. The mono(μ -diphenylsilylene)

(27) (a) Tobita, H.; Kawano, Y.; Shimoi, M.; Ogino, H. *Chem. Lett.* **1987**, 2247–2250. (b) Tobita, H.; Kawano, Y.; Ogino, H. *Chem. Lett.* **1989**, 2155–2158. (c) Ueno, K.; Hamashima, N.; Shimoi, M.; Ogino, H. *Organometallics* **1991**, *10*, 959–962. (d) Kawano, Y.; Tobita, H.; Ogino, H. *J. Organomet. Chem.* **1992**, *428*, 125–143. (e) Kawano, Y.; Tobita, H.; Ogino, H. *Organometallics* **1992**, *11*, 499–500. (f) Kawano, Y.; Tobita, H.; Shimoi, M.; Ogino, H. *J. Am. Chem. Soc.* **1994**, *116*, 8575–8581.

(28) (a) Davison, A.; McCleverty, J. A.; Wilkinson, G. *J. Chem. Soc.* **1963**, 1133–1138. (b) King, R. B.; Iqbal, M. Z.; King, A. D., Jr. *J. Organomet. Chem.* **1979**, *171*, 53–63. (c) Steiner, A.; Gornitzka, H.; Stalke, D.; Edelmann, F. T. *J. Organomet. Chem.* **1992**, *431*, C21–C25.



complex **4a** reacted with CO to afford a mixture of the mono(*μ*-silylene) mono(*μ*-carbonyl) complex {Cp**Ru*(CO)}(*μ*-SiPh₂)(*μ*-CO) (**8**) and the diruthenium tetracarbonyl complex {Cp**Ru*(CO)(*μ*-CO)}₂ (**7**)²⁸ (eq 10). The



ratio between **7** and **8** prior to treatment for purification was 3:10. Complex **8** was fully characterized by means of ¹H, ¹³C, and ²⁹Si NMR, IR, and FD-MS spectroscopy.

In contrast to *cis*-**6a**, only the *trans* isomer was obtained in this reaction. The *trans* form was confirmed by the IR spectrum of **8**. The IR spectrum of **8** exhibited an absorption band at 1910 cm⁻¹. This is the only signal observed in the region of 1800–2100 cm⁻¹ and is ascribed to *ν*_{asym}(CO). In addition, the stretching vibration of the bridging carbonyl group appeared at 1754 cm⁻¹. The ¹³C signals of the carbonyl groups were observed at δ 205.3 and 260.3, which were assigned to the terminal and the bridging carbonyl group, respectively. The ²⁹Si signal of **8** appeared at δ 210.7, which was very similar to that of the dicarbonyl *μ*-silylene complex *cis*-**6a**.

The molecular structure of **8a** is shown in Figure 9, and selected bond distances and angles are listed in Table 6, respectively. Recrystallization of the crude mixture from cold pentane afforded a yellow mixed crystal containing both **7** and **8a** in the ratio of 1:2 in the unit cell. Since **7** has already been structurally

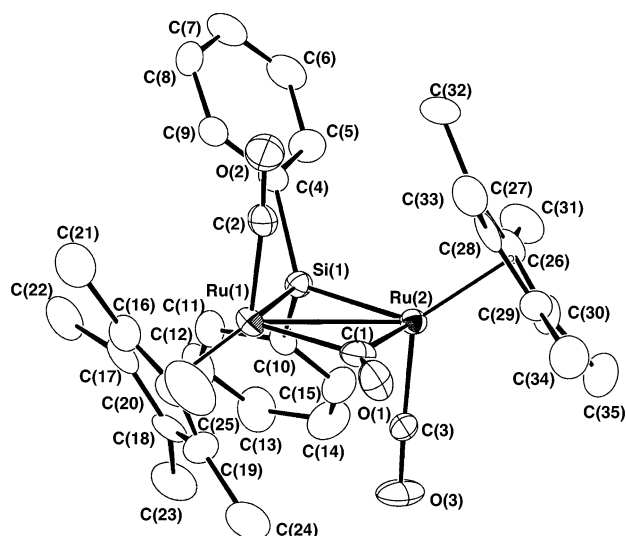


Figure 9. Molecular structure of {Cp**Ru*(CO)}₂(*μ*-SiPh₂)(*μ*-CO) (**8a**), with thermal ellipsoids at the 30% probability level.

Table 6. Selected Bond Distances (Å) and Angles (deg) for **8a**

Ru(1)–Ru(2)	2.846(2)	Ru(1)–Si(1)	2.382(4)
Ru(1)–C(1)	2.04(2)	Ru(1)–C(2)	1.77(2)
Ru(2)–Si(1)	2.385(4)	Ru(2)–C(1)	1.99(2)
Ru(2)–C(3)	1.84(2)	Si(1)–C(4)	1.92(1)
Si(1)–C(10)	1.93(1)	C(1)–O(1)	1.19(2)
C(2)–O(2)	1.20(2)	C(3)–O(3)	1.14(2)
Si(1)–Ru(1)–C(1)	97.6(5)	Si(1)–Ru(2)–C(1)	99.1(5)
Ru(1)–Si(1)–Ru(2)	73.3(1)	C(4)–Si(1)–C(10)	96.8(6)
Ru(1)–C(1)–Ru(2)	89.9(6)	Ru(1)–C(1)–O(1)	132(1)
Ru(2)–C(1)–O(1)	137(1)	Ru(1)–C(2)–O(2)	174(1)
Ru(2)–C(3)–O(3)	178(1)		

characterized,²⁸ only **8a** is shown in Figure 9. The two terminal carbonyl ligands are arranged mutually *trans* with respect to the Ru₂SiC plane.

The Ru–Ru distance of 2.846(2) Å corresponds to an Ru–Ru single bond. The sum of the interior angles of the Ru₂SiC core (359.9°) indicates that these four atoms are located in the same plane. The Ru–Si distance (average 2.38 Å) is slightly longer than those observed in **3a** (2.36 Å) and **4a** (2.35 Å).

The mono(*μ*-silylene) complexes **4b,c** also react with carbon monoxide under forced conditions to afford a mixture of {Cp**Ru*(CO)}(*μ*-SiR₂) (**8b**, R = Me; **8c**, R = Ph) and diruthenium tetracarbonyl complex **7**. Complexes **8b,c** were isolated by means of chromatography on alumina in 17% and 24% yields, respectively. The *trans* geometry of the two CO groups was confirmed on the basis of the ¹H and ¹³C NMR data. The structure of **8c** was confirmed by X-ray diffraction studies. An ORTEP diagram of **8c** is depicted in Figure 10, and selected bond distances and angles are listed in Table 7. Structural parameters of **8c** were very similar to those of **8a**, irrespective of the difference in the substituents on the silicon atom.

Reaction of Bis(*μ*-silylene) Complexes 5 with Acetylene. Reaction of the bis(*μ*-diphenylsilylene) complex **3a** with acetylene afforded the disilaruthenacyclopentene complex {Cp**Ru*(*μ*-H)}₂(–SiPh₂CH=CHSiPh₂) (**9**) (Scheme 6).^{11a} The experiment using deuterated acetylene proved that the disilaruthenacyclopentene skeleton was formed by way of insertion of an acetylene

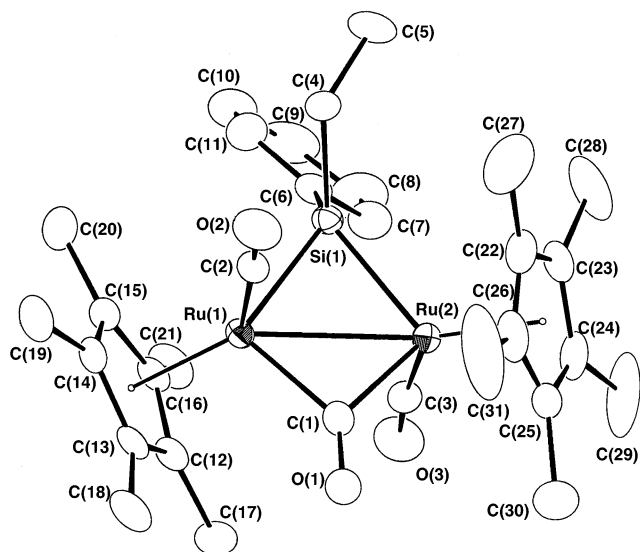


Figure 10. Molecular structure of $\{\text{Cp}^*\text{Ru}(\text{CO})\}_2(\mu\text{-SiPhEt})\text{-}(\mu\text{-CO})$ (**8c**), with thermal ellipsoids at the 30% probability level.

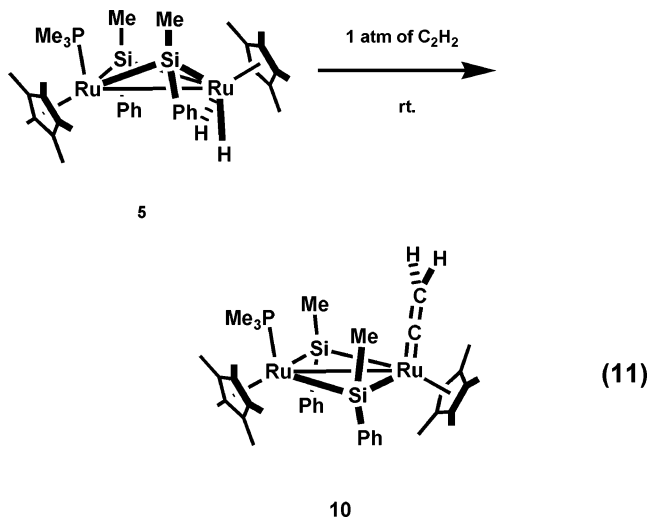
Table 7. Selected Bond Distances (Å) and Angles (deg) for 8c

Ru(1)–Ru(2)	2.848(2)	Ru(1)–Si(1)	2.402(4)
Ru(1)–C(1)	2.016(2)	Ru(1)–C(2)	1.857(7)
Ru(2)–Si(1)	2.389(2)	Ru(2)–C(1)	2.035(2)
Ru(2)–C(3)	1.844(8)	Si(1)–C(4)	1.894(6)
Si(1)–C(6)	1.898(7)	C(1)–O(1)	1.184(7)
C(2)–O(2)	1.148(7)	C(3)–O(3)	1.152(7)
Si(1)–Ru(1)–C(1)	98.7(2)	Si(1)–Ru(2)–C(1)	98.6(2)
Ru(1)–Si(1)–Ru(2)	72.96(6)	C(4)–Si(1)–C(6)	101.4(3)
Ru(1)–C(1)–Ru(2)	89.3(3)	Ru(1)–C(1)–O(1)	135.5(5)
Ru(2)–C(1)–O(1)	135.2(5)	Ru(1)–C(2)–O(2)	175.9(6)
Ru(2)–C(3)–O(3)	173.0(6)		

into the Ru–Si bond. The reaction most likely proceeds via an intermediary *cis*-bis(μ -silylene) complex, in analogy to the reaction of **3b** with PMe_3 . In this regard, the reaction of **3a** with acetylene was another example indicating the existence of the *cis*-bis(μ -silylene) species as well as the reaction with PMe_3 leading to **5**.

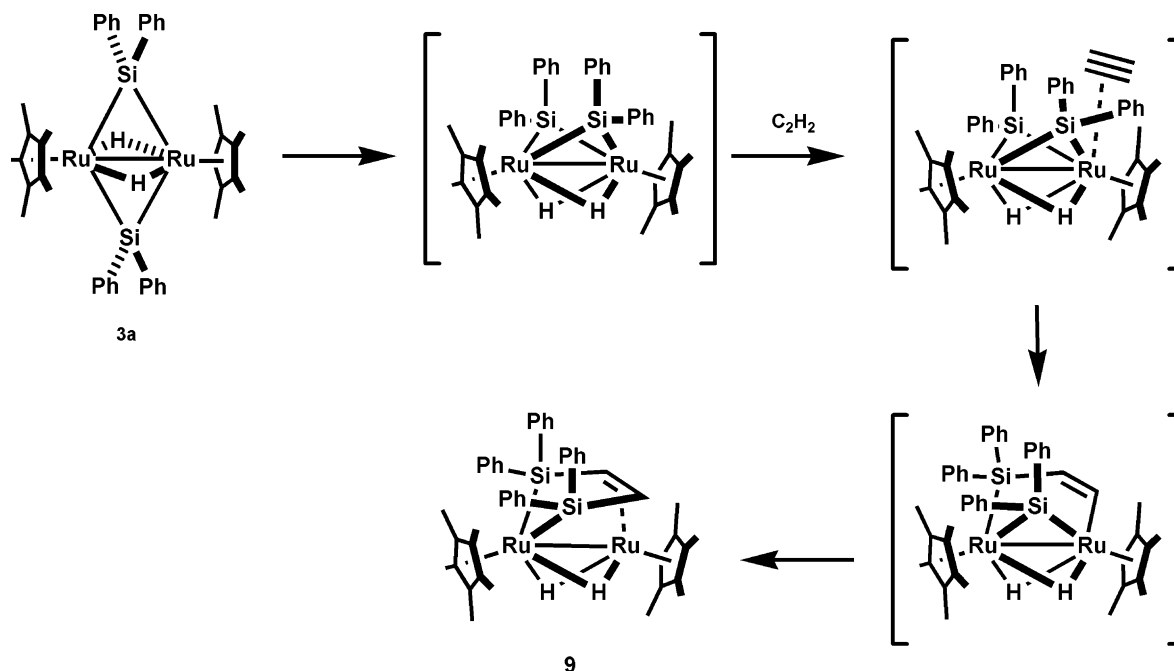
As for complex **5**, the coordination site for the acetylene to insert into the Ru–Si bond has been already occupied by the phosphine. Therefore, the reactivity of **5** should be different from that of the bis(μ -silylene) complex **3** as far as the phosphine coordination to the ruthenium center. Thus, the reaction of **5** with acetylene was investigated to show the role of the coordination site of the *cis*-bis(μ -silylene).

The bis(μ -silylene) complex **5**, containing PMe_3 on one ruthenium center, slowly reacted with acetylene at ambient temperature to yield the vinylidene complex $\{\text{Cp}^*\text{Ru}(\mu\text{-SiPhMe})_2(\text{PMe}_3)(=\text{C}=\text{CH}_2)\}$ (**10**) (eq 11). Complex **10** was fully characterized by means of the ^1H , ^{13}C , and ^{29}Si NMR, IR, and elemental analysis.



The ^{13}C signals derived from the terminally bound vinylidene ligand appeared at δ 327.5 (s, C^α) and δ 91.4 (t, $J_{\text{C-H}} = 160.2$, C^β), respectively. One singlet assignable to the vinylidene proton was observed at δ 3.25 in the ^1H NMR spectrum. The two vinylidene protons were observed to be equivalent, and this is consistent with the terminally bound structure of **10**. In the IR spectra

Scheme 6



of **10**, a strong absorption assignable to $\nu(\text{C}=\text{C})$ was observed at 1593 cm⁻¹.

The *syn* orientation of the two bridging silicon atoms was confirmed by the fact that the two silicon atoms were observed to be equivalent in the ²⁹Si NMR spectra. The ²⁹Si signal of **9** appeared at δ 213.1 as a doublet signal due to coupling with the ³¹P atom (²*J*_{Si-P} = 19.2 Hz). The chemical shift was very close to those of the μ -silylene complexes containing carbonyl ligands, **6** and **8**.

Since a single crystal suitable for the diffraction studies was not obtained, orientation of the two Cp* groups was not determined: that is, whether it is *cis* or *trans* with respect to the Ru₂Si₂ core. However, complex **10** was tentatively identified as a *cis* structure from the analogy to the reaction of **3a** with CO, yielding *cis*-**6a**.

Since the trimethylphosphine was coordinated on one ruthenium center, insertion of acetylene into the Ru–Si bond was inhibited. Although π -coordination of acetylene was required to form the disilaruthenacycle, the reaction of **5** with acetylene leading to the vinylidene complex **10** proceeded by way of C–H bond cleavage of acetylene concomitant with elimination of the two hydride ligands. There have been many examples for the formation of a vinylidene complex via an acetylidene intermediate, and its mechanism has been well elucidated in detail.²⁹

Conclusion

Several complexes containing a μ -silylene ligand, **3–6**, **8**, and **10**, have been synthesized in this study. X-ray diffraction studies revealed that the Ru–Si bonds of these complexes have similar bond lengths. However, a remarkable high-field shift of the ²⁹Si signal was observed only for the bis(μ -silylene) complex **3** in the ²⁹Si NMR studies. Another remarkable property of **3** was its fluxionality; the VT-NMR studies of the mixed-bridge bis(μ -silylene) complex **3c** revealed formation of a μ -silyl intermediate during the site-exchange reaction of the hydride ligands. Actually, the chemical shift of δ 110 for **3** is very close to those of the bis(μ -silyl) complexes **2** containing 2e–3c Ru–H–Si interactions. Therefore, such a high-field shift of the ²⁹Si signal was most likely attributed to the contribution of the resonance hybrid of the μ -silyl structure in solution. In contrast to this, the ²⁹Si signal for the nonfluxional mono(μ -silylene) complex **4** was observed in the low-magnetic-field region (ca. δ 260–310), even though **4** contains hydride ligands.

Consideration of the formal oxidation state of the metal centers is also helpful for understanding the different properties of the silylene bridges in **3** and **4**. The higher formal oxidation state of **3**, which is formally a Ru(IV)–Ru(IV) species, would facilitate rearrangements involving reductive Si–H bond formation into the μ -silyl intermediate.

Another important behavior of the μ -silylene ligand of **3** was the “rotation” around the Ru–Si bonds, which was seen in the isomerization between **3b-syn** and **3b-anti**. The VT-NMR studies of **3c** also proved rotation of the bridging silylene ligand. Rotation of the μ -silylene ligand most likely proceeded by way of a “1,2-shift” of

the intermediary μ -silyl ligand. The kinetic parameters for the hydride site exchange are different from those for the rotation of the μ -silylene ligand, which implied that the two processes took place independently.

Although the X-ray studies of **3a** and **3c** showed *trans* structures of the bis(μ -silylene) complexes with respect to the Ru–Ru vector, the *cis*-bis(μ -silylene) intermediate was proposed for the hydride site-exchange process on the basis of the VT-NMR studies as shown in Scheme 3. The reaction of **3b** with PMe₃ afforded the bis(μ -silylene) complex **5**, whose μ -silylene ligands adopted a *cis* form with respect to the Ru–Ru vector. Thus, formation of **5** strongly implied the transformation of the bis(μ -silylene) complex from *trans* to *cis* in solution. Such transformation from the *trans* to *cis* structure seems to be the origin of the unique reactivities of the bis(μ -silylene) complexes. The mono(μ -silylene) complex **4** has a rigid structure in solution and is less reactive than **3**. It is very helpful for understanding the reactivity of the polyhydride clusters to realize the behavior of the hydride ligands.

We are now continuing research on the reactivities of the μ -silylene ligands on the cluster and are especially focusing on the reactivity of the *cis*-bis(μ -silylene) intermediate for the purpose of formation of Si–C and Si–Si bonds on the cluster.

Experimental Section

General Procedures. All experiments were carried out under an argon atmosphere. All compounds were treated with Schlenk techniques. Reagent grade toluene, Et₂O, and THF were dried over sodium–benzophenone ketyl and stored under an argon atmosphere. Pentane and dichloromethane were dried over phosphorus pentoxide and stored under an argon atmosphere. Benzene-*d*₆, toluene-*d*₈, and THF-*d*₈ were dried over sodium–benzophenone ketyl and stored under an argon atmosphere. Phenylvinylsilane and methylvinylsilane were synthesized by the reduction of the corresponding chlorovinylsilane by LiAlH₄ in diethyl ether. Triphenylsilane, diphenylmethylsilane, phenyldimethylsilane, phenyltrimethylsilane, and other substrates were used as received. IR spectra were recorded on a JASCO FT/IR-5000 spectrophotometer. ¹H and ¹³C NMR spectra were recorded on JEOL GX-500, Varian Gemini-3000, and Varian INOVA-400 Fourier transform spectrometers with tetramethylsilane as an internal standard. Variable-temperature ¹H NMR spectra were recorded on a Varian INOVA-400. ²⁹Si NMR spectra were recorded on JEOL EX-270 and Varian INOVA-400 instruments with tetramethylsilane as an external standard. Field-desorption mass spectra were recorded on a Hitachi GC-MS M80 high-resolution mass spectrometer. Elemental analyses were performed by the Analytical Facility at the Research Laboratory of Resources Utilization, Tokyo Institute of Technology. The dinuclear ruthenium tetrahydride complex (η^5 -C₅Me₅)Ru(μ -H)₄Ru(η^5 -C₅Me₅) (**1**) was prepared according to a previously published method.¹³

X-ray Data Collection and Reduction. X-ray-quality crystal of **3c**, **4a,b**, **5**, and **8a,c** were obtained directly from the preparations described below and mounted on glass fibers. Diffraction experiments were performed on a Rigaku AFC-5R four-circle diffractometer with graphite-monochromated Mo K α radiation (λ = 0.710 69 Å) at 23 °C. Intensity data were collected using a $\omega/2\theta$ scan technique; three standard reflections were recorded every 150 reflections. The data for **4b** and **8a,c** were processed using the TEXSAN crystal solution

(29) Bruce, M. I. *Chem. Rev.* **1991**, *91*, 197–257.

package³⁰ operating on an IRIS Indigo computer, and the data for **3c**, **4a**, and **5** were processed using the SHELX-97 programs.³¹ Neutral atom scattering factors were obtained from the standard sources.³² In the reduction of the data, Lorentz/polarization corrections and empirical adsorption corrections based on azimuthal scans were applied to the data for each structure.

Structure Solution and Refinement for 4b, 8a,c. The Ru atom positions were determined using direct methods employing the MITHRIL-90³³ and SAPI-91³⁴ direct-methods routines for **4b**, and **8a,c**, respectively. In each case the remaining non-hydrogen atoms were located from successive difference Fourier map calculations using the DIRDIF-92 programs.³⁵ In both cases the non-hydrogen atoms were refined anisotropically by using full-matrix least-squares techniques on *F*. In the case of **4b**, the positions of hydrogen atoms bonded to the Ru were located by sequential difference Fourier syntheses and were refined isotropically. Crystal data and results of the analyses are listed in Table 8.

Structure Solution and Refinement for 3c, 4a, and 5. The structure was solved by direct methods using SHELXS-97^{31a} and refined by full-matrix least-squares techniques on *F*² with SHELXL-97.^{31b} All hydrogen atoms were located by difference Fourier maps and refined isotropically, while all non-hydrogen atoms were refined anisotropically. Crystal data and results of the analyses are listed in Table 8.

Variable-Temperature NMR Spectra and Dynamic NMR Simulations. Variable-temperature NMR studies were performed in flame-sealed NMR tubes in THF-*d*₆ for **3b-syn/anti** and toluene-*d*₆ for **3c** using a Varian INOVA-400 Fourier transform spectrometer with tetramethylsilane as an internal standard. NMR simulations for the hydride ligands of **3b-syn** and **3c** were performed using gNMR v4.1.0 (1995–1999 Ivory Soft). In the case of **3c**, simulations for the methyl groups on the bridging silicon atom were also performed. The ¹H–¹H coupling constants between the hydride ligands were estimated at *J*_{H–H} = 6.12 Hz for **3b-syn** and *J*_{H–H} = 6.00 Hz for **3c**, respectively. The coupling constants between the hydrides and the bridging silicon ligand were estimated at ²*J*_{Si–H} = 7.20–9.00 Hz from the line shapes of satellite signals around the resonance of the hydride ligands. Final simulated line shapes were obtained via an iterative parameter search upon the exchange constant *k*. Full details of the fitting procedure may be found in the Supporting Information. The rate constants *k* that accurately modeled the experimental spectra at each temperature are given in Figure 1. The activation parameters Δ*H*[‡] and Δ*S*[‡] were determined from the plot of ln(*k*/*T*) versus 1/*T*. Estimated standard deviations (*σ*) in the slope and *y* intercept of the Eyring plot determined the error in Δ*H*[‡] and Δ*S*[‡], respectively. The standard deviation in Δ*G*[‡] was determined from the formula $\sigma(\Delta G^\ddagger)^2 = \sigma(\Delta H^\ddagger)^2 + [T\sigma(\Delta S^\ddagger)]^2 - 2T\sigma(\Delta H^\ddagger)[\sigma(\Delta S^\ddagger)]$.

Reaction of Cp*Ru(μ-H)₄RuCp* (1) with Ph₃SiH. A 50 mL flask equipped with a dropping funnel was charged with THF (10 mL) and Cp*Ru(μ-H)₄RuCp* (**1**; 0.105 g, 0.22 mmol).

The funnel was charged with triphenylsilane (0.133 g, 0.51 mmol) and THF (10 mL). The Ph₃SiH solution was then slowly added dropwise to the solution of **1** for 5 h. The solution was stirred for 10 h at 25 °C. The solution turned dark red. The solvent was then removed under reduced pressure. Red residual oil containing the bis(μ-diphenylsilylene) complex {Cp*Ru(μ-SiPh₂)(μ-H)₂} (**3a**), the mono(μ-diphenylsilylene) complex {Cp*Ru(μ-H)₂(μ-SiPh₂)} (**4a**), and the remaining triphenylsilane was obtained. After the remaining silane was removed by rinsing with 5 mL of pentane three times, 0.146 g of a red solid including **3a** and **4a** was obtained. The ratio between **3a** and **4a** was estimated at 1:2 by means of ¹H NMR spectroscopy. The residual solid was then dissolved in toluene (15 mL). The solution was transferred to a glass autoclave pressurized with 7 atm of H₂. After the solution was stirred for 30 h at 25 °C, the solvent was removed under reduced pressure. The residual solid was washed seven times with 5 mL of pentane to remove the bis(μ-diphenylsilyl) complex {Cp*Ru(μ-η²-HSiPh₂)}(μ-H)(H) (**2a**). An 80.2 mg amount of complex **4a** was obtained as a dark red solid (56% yield).

Bis(μ-diphenylsilylene) Complex {Cp*Ru(μ-SiPh₂)(μ-H)₂} (3a**).** ¹H NMR (270 MHz, 23 °C, toluene-*d*₆): δ –19.69 (s, 2H, RuH), 1.40 (s, 30H, Cp*), 7.9–7.2 (m, 20H, Ph). ¹³C NMR (68 MHz, 23 °C, benzene-*d*₆): δ 10.8 (q, *J*_{C–H} = 127.0 Hz, C₅Me₅), 90.9 (s, C₅Me₅), 127.3 (d, *J*_{C–H} = 157.8 Hz, Ph), 137.6 (d, *J*_{C–H} = 156.8 Hz, Ph), 145.9 (s, Ph ipso), one ¹³C signal of the phenyl group was obscured by the solvent signals. ²⁹Si{¹H} NMR (54 MHz, 60 °C, benzene-*d*₆): δ 109.8. IR (KBr, cm^{–1}): 3060, 2984, 2910, 1580, 1480, 1429, 1379, 1091, 1031, 732, 699, 512. FD-MS: *m/e* 840. The field desorption mass spectrum was measured, and the intensities of the obtained isotopic peaks for C₄₄H₅₂Ru₂Si₂ agreed with the calculated value within experimental error.

Mono(μ-diphenylsilylene) Complex {Cp*Ru(μ-H)₂(μ-SiPh₂)} (4a**).** ¹H NMR (500 MHz, 23 °C, THF-*d*₆): δ –13.51 (s, 2H, RuH), 1.56 (s, 30H, Cp*), 8.3–7.3 (m, 10H, Ph). ¹³C{¹H} NMR (75 MHz, 23 °C, THF-*d*₆): δ 11.3 (C₅Me₅), 87.3 (C₅Me₅), 128.1 (Ph), 129.3 (Ph), 138.2 (Ph). ²⁹Si{¹H} NMR (54 MHz, 23 °C, benzene-*d*₆): δ 265.0. IR (KBr, cm^{–1}): 3062, 2982, 2904, 1480, 1428, 1382, 1093, 1032, 738, 700. FD-MS: *m/e* 658. The field desorption mass spectrum was measured, and the intensities of the obtained isotopic peaks for C₃₂H₄₂Ru₂Si agreed with the calculated value within experimental error. Anal. Calcd for C₃₂H₄₂Ru₂Si: C, 58.51; H, 6.44. Found: C, 58.14; H, 6.33.

Reaction of Cp*Ru(μ-H)₄RuCp* (1) with Ph₂MeSiH. A 50 mL flask was charged with toluene (20 mL) and Cp*Ru(μ-H)₄RuCp* (**1**; 0.317 g, 0.67 mmol). After 2.5 molar equiv of diphenylmethylsilane (0.34 mL, 1.68 mmol) was added with vigorous stirring, the solution was allowed to react for 12 h at 25 °C. The solvent was then removed under reduced pressure, and the residue was washed two times with 5 mL of methanol to remove the remaining silane. The dark red residual solid was dissolved in 2 mL of toluene, and the product was purified by the use of column chromatography on neutral alumina (Merck Art. 1097) with hexane/toluene. Removal of the solvent under reduced pressure afforded 0.397 g of a mixture of diastereomers of the bis(μ-phenylmethylsilylene) complex {Cp*Ru(μ-SiPhMe)(μ-H)₂} (**3b-syn/anti**) as an orange solid (84%). The ratio between **3b-syn** and **3b-anti** was estimated as 55:45 on the basis of ¹H NMR spectra. ¹H NMR (400 MHz, 60 °C, THF-*d*₆): **3b-syn**, δ –20.4 (br, 2H, RuH), 1.08 (s, 6H, SiMe), 1.529 (s, 30H, Cp*), 7.0–7.5 (m, 10H, Ph); **3b-anti**, δ –20.44 (s, 2H, RuH), 1.12 (s, 6H, SiMe), 1.527 (s, 30H, Cp*), 7.0–7.5 (m, 10H, Ph). ¹H NMR (400 MHz, –40 °C, THF-*d*₆): **3b-syn**, δ –21.01 (d, *J*_{H–H} = 6.1 Hz, 1H, RuH), –19.77 (d, *J*_{H–H} = 6.1 Hz, 1H, RuH), 1.05 (s, 6H, SiMe), 1.50 (s, 30H, Cp*), 6.9–7.8 (m, 10H, Ph); **3b-anti**, δ –20.44 (s, 2H, RuH), 1.09 (s, 6H, SiMe), 1.50 (s, 30H, Cp*), 7.0–7.5 (m, 10H, Ph). ¹³C{¹H} NMR (125 MHz, 23 °C, benzene-*d*₆): δ 5.7 (SiMe), 5.8 (SiMe), 11.5 (C₅Me₅), 11.6 (C₅Me₅), 90.06 (C₅Me₅), 90.10 (C₅–

(30) TEXSAN: Crystal Structure Analysis Package; Molecular Structure Corp., The Woodlands, TX, 1985 and 1992.

(31) (a) Sheldrick, G. M. SHELXS-97: Program for Crystal Structure Solution, University of Göttingen, Göttingen, Germany, 1997. (b) Sheldrick, G. M., SHELXL-97: Program for Crystal Structure Solution; University of Göttingen, Göttingen, Germany, 1997.

(32) *International Tables for X-ray Crystallography*; Kynoch Press: Birmingham, U.K., 1975; Vol. 4.

(33) Gilmore, C. J. MITHRIL 90: MITHRIL-An Integrated Direct Methods Computer Program; University of Glasgow, Glasgow, Scotland, 1990.

(34) Fan, H.-F. SAPI91: Structure Analysis Programs with Intelligent Control; Rigaku Corp., 1991.

(35) Beurskens, P. T.; Admiraal, G.; Beurskens, G.; Bosman, W. P.; Garcia-Granda, S.; Gould, R. O.; Smits, J. M. M.; Smykalla, C. DIRDIF92: The DIRDIF Program System; Technical Report of the Crystallography Laboratory; University of Nijmegen, Nijmegen, The Netherlands, 1992.

Table 8. Crystallographic Data

(a) Compounds 4b and 8a,c			
	4b	8a + 0.5 7	8c
Crystal Parameters			
formula	C ₂₃ H ₄₀ Ru ₂ Si	C ₄₇ H ₅₅ O ₅ Ru ₃ Si	C ₃₁ H ₄₀ O ₃ Ru ₂ Si
cryst syst	monoclinic	triclinic	monoclinic
space group	<i>P2</i> ₁	<i>P</i> $\bar{1}$	<i>P2</i> ₁ / <i>n</i>
<i>a</i> , Å	10.365(3)	11.197(4)	9.464(4)
<i>b</i> , Å	14.220(4)	18.943(5)	16.327(2)
<i>c</i> , Å	8.651(2)	10.954(2)	20.021(4)
α , deg		99.39(2)	
β , deg	104.07(2)	90.02(2)	96.69(3)
γ , deg		75.51(2)	
<i>V</i> , Å ³	1236.7(6)	2217(1)	3072(1)
<i>Z</i>	2	2	4
<i>D</i> _{calcd} , g cm ⁻³	1.468	1.544	1.493
temp, °C	25	23	23
μ (Mo K α), cm ⁻¹	12.75	10.80	10.51
cryst dimens, mm	0.15 × 0.10 × 0.10	0.20 × 0.10 × 0.05	0.30 × 0.25 × 0.20
Data Collection			
diffractometer		Rigaku AFC-5R	
radiation		Mo K α (λ = 0.710 69 Å)	
monochromator		graphite	
scan type		$\omega/2\theta$	
$2\theta_{\max}$, deg	55.0	50.0	50.0
scan speed, deg min ⁻¹	16.0	16.0	16.0
no. of rflns collected	3145	8243	5541
no. of indep data	2959	7809	5182
no. of indep data obsd	2246 (<i>I</i> > 3 σ)	3290 (<i>I</i> > 3 σ)	3130 (<i>I</i> > 3 σ)
Refinement			
<i>R</i>	0.031	0.056	0.036
<i>R</i> _w	0.024	0.046	0.030
<i>p</i> factor	0.00	0.03	0.03
no. of variables	234	505	334
GOF	2.36	1.49	1.33
(b) Compounds 3c , 4a , and 5			
	3c	4a	5
Crystal Parameters			
formula	C ₂₉ H ₄₆ Ru ₂ Si ₂	C ₃₂ H ₄₂ Ru ₂ Si	C ₃₇ H ₅₇ PRu ₂ Si ₂
cryst syst	triclinic	triclinic	monoclinic
space group	<i>P</i> $\bar{1}$	<i>P</i> $\bar{1}$	<i>P2</i> ₁ / <i>n</i>
<i>a</i> , Å	14.602(3)	11.896(2)	11.242(10)
<i>b</i> , Å	18.901(3)	12.345(2)	18.453(11)
<i>c</i> , Å	11.238(4)	10.972(1)	18.065(7)
α , deg	94.45(2)	102.21(1)	
β , deg	90.57(2)	110.744(9)	92.09(5)
γ , deg	99.325(16)	85.23(1)	
<i>V</i> , Å ³	3050.6(13)	1472.8(3)	3745(4)
<i>Z</i>	4	2	4
<i>D</i> _{calcd} , g cm ⁻³	1.422	1.481	1.403
temp, °C	23	23	23
μ (Mo K α), cm ⁻¹	10.83	10.84	9.37
cryst dimens, mm	0.20 × 0.15 × 0.10	0.30 × 0.10 × 0.10	0.10 × 0.15 × 0.10
Data Collection			
diffractometer		Rigaku AFC-5R	
radiation		Mo K α (λ = 0.710 69 Å)	
monochromator		graphite	
scan type		$\omega/2\theta$	
$2\theta_{\max}$, deg		50.0	
scan speed, deg min ⁻¹		16.0	
no. of rflns collected	11 201	5449	7189
no. of indep data	10 727	5178	6825
no. of indep data obsd	6695 (<i>I</i> > 2 σ)	4356 (<i>I</i> > 2 σ)	4267 (<i>I</i> > 2 σ)
Refinement			
R1 [<i>I</i> > 2 σ]	0.0432	0.0355	0.0606
wR2 [<i>I</i> > 2 σ]	0.1017	0.0952	0.1440
no. of params	625	324	402
GOF on <i>F</i> ²	1.002	1.055	1.008

Me₅), 126.9 (SiPh), 127.33 (SiPh), 127.38 (SiPh), 136.9 (SiPh), 149.2 (SiPh-*ipso*), 149.8 (SiPh-*ipso*). Assignment of these ¹³C signals to syn and anti was omitted, and some of these signals for the phenyl carbons were not observed due to obstruction

by the solvent signals. ²⁹Si{¹H} NMR (54 MHz, 23 °C, benzene-*d*₆): δ 108.2, 107.7 (**3b-syn** and/or **3b-anti**). IR (KBr, cm⁻¹): 3062, 2962, 2896, 1481, 1427, 1263, 1121, 1091, 1070, 780, 748, 698. FD-MS: *m/e* 716. The field desorption mass spectrum was

measured, and the intensities of the obtained isotopic peaks for $C_{34}H_{48}Ru_2Si_2$ agreed with the calculated value within experimental error.

Reaction of $Cp^*Ru(\mu-H)_4RuCp^*$ (1**) with $PhMe_2SiH$.** A 50 mL flask was charged with toluene (10 mL) and $Cp^*Ru(\mu-H)_4RuCp^*$ (**1**; 0.149 g, 0.31 mmol). The flask was cooled at $-78^\circ C$ with dry ice/methanol bath. After 2.5 molar equiv of phenyldimethylsilane (0.12 mL, 0.78 mmol) was added with vigorous stirring, the solution was allowed to react for 2 h at $0^\circ C$ with argon bubbling. The solvent and remaining silane were removed under reduced pressure, and 0.212 g of a residual solid including the bis(μ -silylene) complexes $\{Cp^*Ru(\mu-H)_2(\mu-SiPhMe)(\mu-SiMe_2)\}$ (**3c**; >95% based on 1H NMR) and $\{Cp^*Ru(\mu-H)(\mu-SiMe_2)\}$ (**3d**; <2% based on 1H NMR) and their hydrogenated bis(μ -silyl) complexes was obtained. Analytically pure **3c** was obtained from a cold pentane solution of the mixture as a dark red microcrystal.

$\{Cp^*Ru(\mu-H)_2(\mu-SiPhMe)(\mu-SiMe_2)\}$ (3c**).** 1H NMR (400 MHz, $70^\circ C$, THF- d_6): δ -20.80 (s, 2H, RuH), 0.79 (br, 3H, SiMe₂), 0.83 (br, 3H, SiMe₂), 1.01 (s, 3H, SiMePh), 1.68 (s, 30H, Cp*), 7.0–7.3 (m, 5H, SiMePh). 1H NMR (400 MHz, $-60^\circ C$, THF- d_6): δ -21.13 (d, $J_{H-H} = 6.0$ Hz, 1H, RuH), -20.44 (d, $J_{H-H} = 6.0$ Hz, 1H, RuH), 0.74 (s, 3H, SiMe₂), 0.79 (br, 3H, SiMe₂), 0.97 (s, 3H, SiMePh), 1.65 (s, 30H, Cp*), 6.7–7.7 (m, 5H, SiMePh). $^{13}C\{^1H\}$ NMR (75 MHz, $23^\circ C$, benzene- d_6): δ 5.5 (SiMe), 9.8 (SiMe), 10.0 (SiMe), 11.8 (C_5Me_5), 90.1 (C_5Me_5), 137.2 (br, Ph), 149.9 (Ph-*ipso*). $^{29}Si\{^1H\}$ NMR (54 MHz, $23^\circ C$, benzene- d_6): δ 112.3 (SiMe₂), 107.9 (SiPhMe). FD-MS: *m/e* 654. The field desorption mass spectrum was measured, and the intensities of the obtained isotopic peaks for $C_{29}H_{46}Ru_2Si_2$ agreed with the calculated value within experimental error. Anal. Calcd for $C_{29}H_{46}Ru_2Si_2$: C, 53.34; H, 7.10. Found: C, 51.45; H, 6.90.

$\{Cp^*Ru(\mu-H)(\mu-SiMe_2)\}$ (3d**).** 1H NMR (400 MHz, $-60^\circ C$, THF- d_6): δ -21.16 (s, 2H, RuH), 0.66 (s, 12H, SiMe), 1.78 (s, 30H, Cp*). FD-MS: *m/e* 594. The field desorption mass spectrum was measured, and the intensities of the obtained isotopic peaks for $C_{24}H_{46}Ru_2Si_2$ agreed with the calculated value within experimental error.

Preparation of $\{Cp^*Ru(\mu-H)_2(\mu-SiPhEt)\}$ (4b**).** A 50 mL flask equipped with a dropping funnel was charged with toluene (20 mL) and $Cp^*Ru(\mu-H)_4RuCp^*$ (**1**; 0.665 g, 1.39 mmol). The funnel was charged with phenylvinylsilane (0.525 mL, 0.51 mmol) and toluene (25 mL). The $PhSi(CH=CH_2)_2H_2$ solution was then slowly added dropwise to the solution of **1** for 1 h. The solution was stirred for 1 h at $25^\circ C$. The solvent was then removed under reduced pressure. After the remaining silane was removed by rinsing with 5 mL of pentane three times, **4b** was obtained as a red solid (0.570 g, 0.94 mmol, 67% yield). 1H NMR (500 MHz, $23^\circ C$, benzene- d_6): δ -13.43 (d, $J_{H-H} = 3.9$ Hz, 1H, RuH), -13.41 (d, $J_{H-H} = 3.9$ Hz, 1H, RuH), 1.66 (s, 30H, Cp*), 1.70 (q, $J_{H-H} = 7.4$ Hz, 2H, SiCH₂), 1.83 (t, $J_{H-H} = 7.4$ Hz, 3H, SiCH₂CH₃), 7.3–8.4 (m, 5H, SiPh). ^{13}C NMR (125 MHz, $23^\circ C$, benzene- d_6): δ 11.0 (q, $J_{C-H} = 124.0$ Hz, SiCH₂CH₃), 11.6 (q, $J_{C-H} = 126.5$ Hz, C_5Me_5), 18.1 (t, $J_{C-H} = 115.4$ Hz, SiCH₂CH₃), 86.2 (s, C_5Me_5), 127.5 (Ph), 128.8 (Ph), 136.4 (Ph), 150.1 (Ph-*ipso*). $^{29}Si\{^1H\}$ NMR (54 MHz, $23^\circ C$, benzene- d_6): δ 291.7. IR (KBr, cm^{-1}): 2980, 2956, 2900, 1479, 1431, 1383, 1094, 1038, 692. FD-MS: *m/e* 610. The field desorption mass spectrum was measured, and the intensities of the obtained isotopic peaks for $C_{28}H_{42}Ru_2Si$ agreed with the calculated value within experimental error. Anal. Calcd for $C_{28}H_{42}Ru_2Si$: C, 55.24; H, 6.95. Found: C, 55.25; H, 7.22.

Preparation of $\{Cp^*Ru(\mu-H)_2(\mu-SiMeEt)\}$ (4c**).** A 50 mL flask equipped with a dropping funnel was charged with toluene (30 mL) and $Cp^*Ru(\mu-H)_4RuCp^*$ (**1**) (0.581 g, 1.22 mmol). The funnel was charged with methylvinylsilane (0.286 mL, 2.68 mmol) and toluene (40 mL). The $MeSi(CH=CH_2)_2H_2$ solution was then slowly added dropwise to the solution of **1** for 3.5 h. The solution was stirred for 2 h at $25^\circ C$. The solvent was then removed under reduced pressure. After the remain-

ing silane was removed by rinsing with 5 mL of pentane three times, **4c** was obtained as a red solid (0.185 g, 0.34 mmol, 28% yield). 1H NMR (300 MHz, $23^\circ C$, benzene- d_6): δ -14.69 (d, $J_{H-H} = 3.7$ Hz, 1H, RuH), -14.60 (d, $J_{H-H} = 3.7$ Hz, 1H, RuH), 1.32 (s, 3H, SiCH₃), 1.43 (q, $J_{H-H} = 7.7$ Hz, 2H, SiCH₂), 1.71 (t, $J_{H-H} = 7.4$ Hz, 3H, SiCH₂CH₃), 1.77 (s, 30H, Cp*). ^{13}C NMR (75 MHz, $23^\circ C$, benzene- d_6): δ 11.6 (q, $J_{C-H} = 123.4$ Hz, SiCH₂CH₃), 11.8 (q, $J_{C-H} = 126.6$ Hz, C_5Me_5), 17.5 (q, $J_{C-H} = 118.8$ Hz, SiCH₃), 24.3 (t, $J_{C-H} = 116.6$ Hz, SiCH₂CH₃), 85.8 (s, C_5Me_5). $^{29}Si\{^1H\}$ NMR (54 MHz, $23^\circ C$, benzene- d_6): δ 310.8. IR (KBr, cm^{-1}): 2980, 2960, 2896, 1477, 1402, 1379, 1226, 1031, 785, 679, 623. Anal. Calcd for $C_{23}H_{40}Ru_2Si$: C, 50.52; H, 7.37. Found: C, 50.91; H, 7.39.

Preparation of $\{Cp^*Ru(\mu-SiPhMe)_2(PMe_3)(H)_2\}$ (5**).** A 50 mL flask was charged with toluene (10 mL) and $\{Cp^*Ru(\mu-SiPhMe)(\mu-H)\}_2$ (**3b-syn/anti**) (0.222 g, 0.31 mmol). After 2.5 molar equiv of trimethylphosphine (1.58 M/toluene; 0.5 mL, 0.79 mmol) was added with vigorous stirring, the reaction mixture was stirred for 24 h at $25^\circ C$. The solution turned from dark red to orange. After the solvent and remaining PMe_3 were removed under reduced pressure, a yellow residual solid was obtained. This solid was dissolved in 5 mL of pentane, and the product was purified by the use of filtration on Celite. Removal of the solvent in vacuo afforded 0.200 g of **5** as a yellow solid (82% yield). 1H NMR (500 MHz, $23^\circ C$, toluene- d_8): δ -13.06 (s, 2H, RuH), 1.01 (d, $J_{P-H} = 1.2$ Hz, 6H, SiMe), 1.20 (d, $J_{P-H} = 0.7$ Hz, 15H, Cp*), 1.5–1.1 (br, 9H, PMe_3), 1.84 (s, 15H, Cp*), 7.3–8.3 (m, 10H, SiPh). 1H NMR (500 MHz, $-40^\circ C$, toluene- d_8): δ -12.99 (s, 2H, RuH), 1.02 (s, 6H, SiMe), 1.11 (d, $J_{P-H} = 7.9$ Hz, 3H, PMe), 1.18 (s, 15H, Cp*), 1.35 (d, $J_{P-H} = 7.9$ Hz, 3H, PMe), 1.80 (s, 15H, Cp*), 7.3–8.4 (m, 10H, SiPh). $^{13}C\{^1H\}$ NMR (75 MHz, $23^\circ C$, benzene- d_6): δ 11.2 (C_5Me_5), 11.8 (C_5Me_5), 19.0 (d, $J_{P-C} = 1.4$ Hz, SiMe), 25.7 (br, PMe), 94.7 (C_5Me_5), 94.8 (C_5Me_5), 127.1 (SiPh), 127.4 (SiPh), 136.5 (SiPh), 155.2 (SiPh-*ipso*). $^{29}Si\{^1H\}$ NMR (54 MHz, $23^\circ C$, benzene- d_6): δ 205.2 (d, $J_{P-Si} = 20.5$ Hz). $^{31}P\{^1H\}$ NMR (109 MHz, $23^\circ C$, benzene- d_6): δ 16.6. IR (KBr, cm^{-1}): 3128, 3040, 3000, 2960, 2904, 2856, 2720, 2036 (ν (Ru–H)), 1957, 1889, 1827, 1580, 1562, 1425, 1377, 1276, 1261, 1083, 1025, 944, 779, 735. Anal. Calcd for $C_{37}H_{57}PRu_2Si_2$: C, 56.17; H, 7.26. Found: C, 56.16; H, 7.51.

Thermolysis of $\{Cp^*Ru(\mu-SiPhMe)_2(PMe_3)(H)_2\}$ (5**).** Complex **5** (10 mg, 0.013 mmol) was dissolved in benzene- d_6 (0.3 mL), and then the solution was charged in an NMR tube. The NMR tube was then heated at $100^\circ C$ for 10 h. The 1H NMR spectrum revealed complete disappearance of **5** and formation of a mixture of **3b-syn/anti** and trimethylphosphine (δ 0.83, $J_{P-H} = 12.8$ Hz).

Reaction of $\{Cp^*Ru(\mu-SiPh_2)(\mu-H)_2\}$ (3a**) with H_2 .** Toluene (20 mL) and complex **3a** (0.125 g, 0.15 mmol) was charged in a 100 mL flask under 1 atm of H_2 . After the solution was stirred for 48 h at $25^\circ C$, the solution turned orange. The bis(μ -diphenylsilyl) complex $\{Cp^*Ru(\mu-\eta^2-HSiPh_2)_2(\mu-H)(H)\}$ (**2a**) was obtained as an orange solid by the removal of the solvent under reduced pressure (0.125 g, 100% yield). $^{29}Si\{^1H\}$ NMR (54 MHz, $23^\circ C$, benzene- d_6): δ 95.1.

Reaction of $\{Cp^*Ru(\mu-SiPhMe)(\mu-H)_2\}$ (3b-syn/anti**) with H_2 .** Toluene (10 mL) and a mixture of **3b-syn** and **3b-anti** (0.155 g, 0.22 mmol) was charged in a 100 mL flask under 1 atm of H_2 . After the solution was stirred for 8 h at $25^\circ C$, the solution turned orange. A mixture of bis(μ -phenylmethylsilyl) complexes $\{Cp^*Ru(\mu-\eta^2-HSiPhMe)_2(\mu-H)(H)\}$ (**2b-syn/anti**) was obtained as a yellow solid by removal of the solvent under reduced pressure (0.155 g, 100% yield).

Isolation of **2b-syn.** The product was extracted with seven 5 mL portions of pentane, and the combined extract was evaporated. The yellow residual solid was then dissolved in 3 mL of toluene and purified by the use of column chromatography on neutral silica gel (Merck Art. 7734) and alumina (Merck Art. 1097) with hexane. Removal of the solvent under reduced pressure afforded **2b-syn** as a yellow solid (0.065 g,

42% yield). ¹H NMR (500 MHz, -80 °C, THF-*d*₆): δ -15.17 (s, 1H, Ru μ Ru or Ru μ H), -12.89 (s, 2H, Ru μ HSi), -12.15 (s, 1H, Ru μ Ru or Ru μ H), 0.66 (s, 6H, SiMe), 2.00 (s, 15H, Cp*), 2.04 (s, 15H, Cp*), 7.0–7.3 (m, 10H, SiPh). ¹³C NMR (126 MHz, 30 °C, THF-*d*₆): δ 11.1 (q, *J*_{C-H} = 120.2 Hz, SiCH₃), 13.7 (q, *J*_{C-H} = 126.3, C₅Me₅), 95.6 (s, C₅Me₅), 128.5 (d, *J*_{C-H} = 150.7 Hz, SiPh), 128.6 (d, *J*_{C-H} = 163.1 Hz, SiPh), 135.8 (d, *J*_{C-H} = 157.4 Hz, SiPh), 151.2 (s, SiPh-*ipso*). ²⁹Si{¹H} NMR (54 MHz, 23 °C, benzene-*d*₆): δ 101.9. IR (KBr, cm⁻¹): 3068, 2956, 2908, 2064 (ν(Ru-H)), 1944, 1882, 1814, 1748 br (ν(Ru-H-Si)), 1425, 1377, 1230, 1094, 1029, 787, 733, 698, 673. FD-MS: *m/e* 718. The field desorption mass spectrum was measured, and the intensities of the obtained isotopic peaks for C₃₄H₅₀Ru₂Si₂ agreed with the calculated value within experimental error. Anal. Calcd for C₃₄H₅₀Ru₂Si₂: C, 56.95; H, 7.03. Found: C, 57.53; H, 6.91.

Isolation of 2b-anti. The product was washed by 5 mL of pentane seven times. Decantation and removal of the solvent under reduced pressure afforded **2b-anti** as a yellow solid (0.045 g, 30% yield). ¹H NMR (500 MHz, -80 °C, THF-*d*₆): δ -14.98 (br, 1H, RuH), -13.45 (br, 1H, RuH), -13.07 (br, 1H, RuH), -12.42 (br, 1H, RuH), 0.34 (s, 3H, SiMe), 0.66 (s, 3H, SiMe), 1.84 (br, 15H, Cp*), 1.93 (br, 15H, Cp*), 7.1–7.7 (m, 10H, SiPh). ¹³C{¹H} NMR (126 MHz, -50 °C, THF-*d*₆): δ 8.3 (SiMe), 10.5 (SiMe), 12.4 (C₅Me₅), 94.2 (s, C₅Me₅), 127.2 (SiPh), 127.7 (SiPh), 134.8 (SiPh), 136.2 (SiPh), other signals derived from phenyl groups were not observed due to the fluxionality of **2b-anti**. IR (KBr, cm⁻¹): 3062, 2978, 2910, 2094 (ν(Ru-H)), 1965, 1837, 1823, 1739 br (ν(Ru-H-Si)), 1427, 1379, 1228, 1091, 1029, 785, 735, 698, 673. FD-MS: *m/e* 718. The field desorption mass spectrum was measured, and the intensities of the obtained isotopic peaks for C₃₄H₅₀Ru₂Si₂ agreed with the calculated value within experimental error. Anal. Calcd for C₃₄H₅₀Ru₂Si₂: C, 56.95; H, 7.03. Found: C, 57.53; H, 6.91.

Reaction of {Cp*Ru(μ-H)}₂(μ-SiMe₂)(μ-SiPhMe) (3c) with H₂. Toluene (10 mL) and the crude product of the reaction of **1** with PhMe₂SiH (0.0994 g), which included {Cp*Ru(μ-H)}(μ-SiMe₂)(μ-SiPhMe) (**3c**) in 80% yield, were charged in a 50 mL reaction flask. After the reaction vessel was degassed, 1 atm of H₂ was introduced into the flask. The solution was vigorously stirred for 2 h at 25 °C. The solvent was then removed at reduced pressure, and a brownish residual solid including the bis(μ-silyl) complex (Cp*Ru)₂(μ-η²-HSiMe₂)(μ-η²-HSiPhMe)(μ-H)(H) (**2c**) in 80% yield was obtained (0.1040 g). Isolation of **2c** by the use of column chromatography failed due to decomposition on alumina; thus, formation of **2c** was confirmed on the basis of ¹H NMR spectral data of the crude product. ¹H NMR (400 MHz, 23 °C, THF-*d*₆): δ -13.59 (br, 4H, RuH and RuHSi), 0.15 (br, 3H, SiMe₂), 0.41 (br, 3H, SiMe₂), 0.60 (s, 3H, SiMePh), 2.02 (br, 30H, Cp*), 7.0–7.5 (m, 5H, SiMePh). ¹H NMR (400 MHz, -95 °C, THF-*d*₆): δ -15.22 (s, 1H, RuH), -13.50 (s, ²*J*_{Si-H} = 44 Hz, 1H, RuHSi), -13.16 (s, ²*J*_{Si-H} = 44 Hz, 1H, RuHSi), 12.59 (s, 1H, RuH), 0.18 (s, 3H, SiMe₂), 0.37 (s, 3H, SiMe₂), 0.58 (s, 3H, SiMePh), 1.97 (s, 15H, Cp*), 2.04 (s, 15H, Cp*), 7.1–7.5 (m, 5H, SiMePh).

Reaction of {Cp*Ru(μ-H)}₂(μ-SiPh₂) (4a) with H₂. Toluene (10 mL) and {Cp*Ru(μ-H)}₂(μ-SiPh₂) (**4a**; 0.020 g, 0.030 mmol) were charged in a 50 mL glass autoclave. After the reaction vessel was degassed, 7 atm of H₂ was introduced. The reaction vessel was heated at 100 °C for 24 h. The solvent was then evaporated under reduced pressure, and 0.018 g of a dark reddish residual solid including Cp*Ru(μ-H)₄RuCp* (**1**), {Cp*Ru(μ-H)}₃(μ₃-H)₂, and (Cp*Ru)₄(H)₆ was obtained. The ratio among them was estimated as 32:65:3 on the basis of ¹H NMR spectra. ¹H NMR (400 MHz, 23 °C, benzene-*d*₆): Cp*Ru(μ-H)₄RuCp* (**1**), δ -13.98 (s, 4H, RuH), 1.87 (s, 30H, Cp*); {Cp*Ru(μ-H)}₃(μ₃-H)₂, δ -7.24 (s, 5H, RuH), 2.03 (s, 45H, Cp*); (Cp*Ru)₄(H)₆, δ -9.32 (s, 6H, RuH), 1.90 (s, 60H, Cp*).

Preparation of {Cp*Ru(μ-SiPh₂)(CO)}₂ (cis-6a). Toluene (10 mL) and {Cp*Ru(μ-SiPh₂)(μ-H)}₂ (**3a**; 32.0 mg, 0.038 mmol)

were charged in a glass autoclave with 5 atm of carbon monoxide. The solution was stirred for 20 h at 25 °C. The solution turned bright yellow from dark red. Removal of the solvent under reduced pressure afforded 34.0 mg of **cis-6a** as a yellow solid (100% yield). ¹H NMR (270 MHz, 23 °C, dichloromethane-*d*₂): δ 1.52 (s, 30H, Cp*), 7.0–7.7 (m, 20H, SiPh). ¹³C NMR (68 MHz, 23 °C, dichloromethane-*d*₂): δ 10.7 (q, *J*_{C-H} = 127.0 Hz, C₅Me₅), 99.0 (s, C₅Me₅), 126.7 (d, *J*_{C-H} = 156.7 Hz, SiPh), 127.3 (d, *J*_{C-H} = 154.7 Hz, SiPh), 127.7 (d, *J*_{C-H} = 158.9 Hz, SiPh), 128.3 (d, *J*_{C-H} = 158.8 Hz, SiPh), 135.2 (d, *J*_{C-H} = 158.8 Hz, SiPh), 147.6 (s, SiPh-*ipso*), 152.2 (s, SiPh-*ipso*), 205.2 (s, CO). ²⁹Si{¹H} NMR (54 MHz, 23 °C, benzene-*d*₆): δ 211.4. IR (KBr, cm⁻¹): 3046, 2970, 2910, 1955 (ν(CO)), 1922 sh, 1480, 1425, 1380, 1263, 1078, 1019, 807, 701. FD-MS: *m/e* 894. The field desorption mass spectrum was measured, and the intensities of the obtained isotopic peaks for C₄₆H₅₀O₂Ru₂Si₂ agreed with the calculated value within experimental error. Anal. Calcd for C₄₆H₅₀O₂Ru₂Si₂: C, 61.86; H, 5.64. Found: C, 61.63; H, 5.59.

Preparation of {Cp*Ru(μ-SiPhMe)(CO)}₂ (6b). Toluene (10 mL) and {Cp*Ru(μ-SiPhMe)(μ-H)}₂ (**3b-syn/anti**; 0.101 g, 0.14 mmol) were charged in a glass autoclave with 5 atm of carbon monoxide. The solution was stirred for 20 h at 25 °C. The solution turned bright yellow from dark red. Removal of the solvent under reduced pressure afforded a yellow residual oil containing **cis-6b-syn**, **trans-6b-anti**, {Cp*Ru(CO)(μ-CO)}₂ (**7**), and other unidentified byproducts. The complex **cis-6b-syn** was extracted with five 5 mL portions of pentane to remove **7**, and the combined extract was purified by the use of column chromatography on silica gel (Merck Art. 7734) with hexane/toluene after condensation. Removal of the solvent in vacuo afforded **cis-6b-syn** as a yellow solid (0.075 g, 70% yield). ¹H NMR (300 MHz, 23 °C, benzene-*d*₆): δ 1.36 (s, 30H, Cp*), 1.55 (s, 6H, SiMe), 7.2–7.5 (m, 10H, SiPh). ¹³C{¹H} NMR (68 MHz, 23 °C, benzene-*d*₆): δ 6.2 (SiMe), 9.0 (C₅Me₅), 96.7 (s, C₅Me₅), 135.7 (SiPh), 152.0 (SiPh-*ipso*), 205.6 (s, CO). IR (KBr, cm⁻¹): 3064, 2962, 2896, 1932 (ν(CO)), 1903 sh, 1431, 1379, 1265, 1094, 1021, 789. Anal. Calcd for C₃₆H₄₆O₂Ru₂Si₂: C, 56.22; H, 6.03. Found: C, 55.84; H, 6.22. The complex **trans-6b-anti** was obtained as a yellow microcrystal by recrystallization of the dilute pentane solution of the mixture at -20 °C (0.015 mg, 14%). ¹H NMR (300 MHz, 23 °C, benzene-*d*₆): δ 1.41 (s, 6H, SiMe), 1.58 (s, 30H, Cp*), 7.2–8.0 (m, 10H, SiPh). ¹³C{¹H} NMR (68 MHz, 23 °C, benzene-*d*₆): δ 10.6 (C₅Me₅), 11.9 (SiMe), 96.7 (s, C₅Me₅), 127.1 (SiPh), 128.2 (SiPh), 135.6 (SiPh), 149.2 (SiPh-*ipso*), 205.5 (CO). IR (KBr, cm⁻¹): 2898, 1899 (ν(CO)), 1477, 1427, 1379, 1261, 1236, 1087, 1029, 793.

Preparation of {Cp*Ru(CO)}(μ-SiPhMe)(μ-SiMe₂) (trans-6c). Toluene (10 mL) and {Cp*Ru(μ-H)}₂(μ-SiPhMe)(μ-SiMe₂) (**3c**; 0.145 g, 0.22 mmol) were charged in a glass autoclave with 5 atm of carbon monoxide. The solution was stirred for 5 h at 120 °C. The solution turned bright yellow from red. Removal of the solvent under reduced pressure afforded a yellow residual oil containing **trans-6c**, {Cp*Ru(CO)(μ-CO)}₂ (**7**), and other unidentified byproducts. The products were dissolved in 4 mL of pentane and purified by the use of column chromatography on neutral alumina (Merck Art. 1097) with hexane. Removal of the solvent in vacuo afforded **trans-6c** as a yellow solid (0.046 g, 37% yield). ¹H NMR (300 MHz, 23 °C, benzene-*d*₆): δ 1.08 (s, 3H, SiMe), 1.14 (s, 3H, SiMe), 1.34 (s, 3H, SiMe), 1.61 (s, 15H, Cp*), 1.74 (s, 15H, Cp*), 7.2–8.0 (m, 5H, SiPh). IR (KBr, cm⁻¹): 2978, 2908, 1903 (ν(CO)), 1479, 1427, 1379, 1263, 1236, 1089, 1071, 841, 793, 768, 663.

Preparation of {Cp*Ru(CO)}(μ-SiPh₂)(μ-CO) (8a). Toluene (10 mL) and {Cp*Ru(μ-H)}₂(μ-SiPh₂) (**4a**; 0.074 g, 0.11 mmol) were charged in a glass autoclave with 8 atm of carbon monoxide. The solution was stirred for 6 h at 100 °C. The color of the solution turned bright yellow from dark red. Removal of the solvent under reduced pressure afforded a yellow residual solid containing **8a** and {Cp*Ru(CO)(μ-CO)}₂ (**7**) in

the ratio of 10:3. The product was dissolved in 4 mL of toluene and purified by the use of column chromatography on neutral alumina (Merck Art. 1097) with hexane/toluene. Removal of the solvent in vacuo afforded **8a** as a yellow solid (0.044 g, 54% yield). Recrystallization of the crude mixture from the cold pentane solution afforded a mixed crystal including **8a** and **7** in the ratio of 2:1. ^1H NMR (300 MHz, 23 °C, benzene- d_6): δ 1.63 (s, 30H, Cp*), 7.2–8.0 (m, 10H, SiPh). $^{13}\text{C}\{^1\text{H}\}$ NMR (76 MHz, 23 °C, benzene- d_6): δ 9.8 (C_5Me_5), 100.3 (C_5Me_5), 127.5 (SiPh), 128.9 (SiPh), 138.3 (SiPh), 150.1 (SiPh-*ipso*), 205.3 (CO), 260.3 (μ -CO). $^{29}\text{Si}\{^1\text{H}\}$ NMR (54 MHz, 23 °C, benzene- d_6): δ 210.7. IR (KBr, cm^{-1}): 3054, 2988, 2962, 2912, 1916 ($\nu(\text{CO})$), 1754 ($\nu(\mu\text{-CO})$), 1481, 1427, 1381, 1085, 1031, 841, 702, 642. FD-MS: *m/e* 740. The field desorption mass spectrum was measured, and the intensities of the obtained isotopic peaks for $\text{C}_{35}\text{H}_{40}\text{O}_3\text{Ru}_2\text{Si}$ agreed with the calculated value within experimental error.

Preparation of $\{\text{Cp}^*\text{Ru}(\text{CO})\}(\mu\text{-SiMeEt})(\mu\text{-CO})$ (8b**).** Toluene (10 mL) and $\{\text{Cp}^*\text{Ru}(\mu\text{-H})_2(\mu\text{-SiMeEt})\}$ (**4b**; 0.074 g, 0.14 mmol) were charged in a glass autoclave with 8 atm of carbon monoxide. The solution was stirred for 13 h at 110 °C. The color of the solution turned bright yellow from dark red. Removal of the solvent under reduced pressure afforded a yellow residual solid, and the product was dissolved in 4 mL of toluene. The products was dissolved in 4 mL of pentane and purified by the use of column chromatography on neutral alumina (Merck Art. 1097) with hexane/toluene. Removal of the solvent in vacuo afforded **8b** as a yellow solid (0.015 g, 17% yield). ^1H NMR (300 MHz, 23 °C, benzene- d_6): δ 1.23 (s, 3H, SiMe), 1.49 (t, 3H, $J_{\text{H-H}} = 7.2$ Hz, SiCH_2CH_3), 1.77 (s, 15H, Cp*), 1.79 (s, 15H, Cp*), 1.82 (q, $J_{\text{H-H}} = 7.2$ Hz, SiCH_2CH_3).

Preparation of $\{\text{Cp}^*\text{Ru}(\text{CO})\}(\mu\text{-SiPhEt})(\mu\text{-CO})$ (8c**).** Toluene (10 mL) and $\{\text{Cp}^*\text{Ru}(\mu\text{-H})_2(\mu\text{-SiPh}_2)\}$ (**4a**; 0.070 g, 0.10 mmol) were charged in a glass autoclave with 8 atm of carbon monoxide. The solution was stirred for 4 h at 110 °C. The color of the solution turned bright yellow from dark red. Removal of the solvent under reduced pressure afforded a yellow residual solid. The product was dissolved in 4 mL of toluene and purified by the use of column chromatography on neutral alumina (Merck Art. 1097) with hexane/toluene. Removal of the solvent in vacuo afforded **8c** as a yellow solid (0.025 g, 24% yield). ^1H NMR (300 MHz, 23 °C, benzene- d_6): δ 1.55 (t, 3H, $J_{\text{H-H}} = 7.7$ Hz, SiCH_2CH_3), 1.64 (s, 15H, Cp*), 1.80 (s, 15H, Cp*), 1.94 (q, $J_{\text{H-H}} = 7.7$ Hz, SiCH_2CH_3), 7.2–8.1 (m, 5H, SiPh). $^{13}\text{C}\{^1\text{H}\}$ NMR (76 MHz, 23 °C, benzene- d_6): δ 9.9

(C_5Me_5), 10.4 (C_5Me_5), 12.0 (SiEt), 20.6 (SiEt), 100.1 (C_5Me_5), 100.3 (C_5Me_5), 127.8 (SiPh), 128.9 (SiPh), 136.4 (SiPh), 147.9 (SiPh-*ipso*), 204.1 (CO), 204.4 (CO), 262.1 (μ -CO). $^{29}\text{Si}\{^1\text{H}\}$ NMR (54 MHz, 23 °C, benzene- d_6): δ 216.2. IR (KBr, cm^{-1}): 3066, 2958, 2902, 2870, 1910 ($\nu(\text{CO})$), 1767 ($\nu(\mu\text{-CO})$), 1481, 1427, 1381, 1261, 1093, 1069, 1031, 696. Anal. Calcd for $\text{C}_{31}\text{H}_{40}\text{O}_3\text{Ru}_2\text{Si}$: C, 53.89; H, 5.84. Found: C, 54.19; H, 6.17.

Preparation of $\{\text{Cp}^*\text{Ru}(\mu\text{-SiPhMe})_2(\text{PMe}_3)(=\text{C}=\text{CH}_2)\}$ (10**).** Toluene (10 mL) and $\{\text{Cp}^*\text{Ru}(\mu\text{-SiPhMe})_2(\text{PMe}_3)(\text{H})_2\}$ (**5**; 0.209 g, 0.26 mmol) were charged in a 50 mL flask with 1 atm of acetylene. The solution was stirred for 2 days at 25 °C. Removal of the solvent under reduced pressure afforded 0.193 g of a brown solid including **10** in 80% yield (based on ^1H NMR). Analytically pure **10** was obtained by recrystallization from cold pentane solution. ^1H NMR (500 MHz, 23 °C, benzene- d_6): δ 0.96 (s, 6H, SiMe), 1.35 (d, $J_{\text{H-P}} = 1.3$ Hz, 15H, Cp*), 1.37 (d, $J_{\text{H-P}} = 8.0$ Hz, 9H, PMe), 1.74 (s, 15H, Cp*), 3.25 (s, 2H, $=\text{C}=\text{CH}_2$), 7.2–7.8 (m, 10H, SiPh). ^{13}C NMR (68 MHz, 23 °C, benzene- d_6): δ 11.07 (q, $J_{\text{C-H}} = 126.8$ Hz, C_5Me_5), 11.09 (q, $J_{\text{C-H}} = 126.8$ Hz, C_5Me_5), 18.0 (dq, $J_{\text{C-H}} = 119.2$ Hz, $J_{\text{P-C}} = 5.7$ Hz, SiMe), 24.3 (dq, $J_{\text{C-H}} = 128.8$ Hz, $J_{\text{P-C}} = 27.7$ Hz, PMe), 91.4 (t, $J_{\text{C-H}} = 160.2$ Hz, $=\text{C}=\text{CH}_2$), 94.2 (s, C_5Me_5), 98.4 (s, C_5Me_5), 126.7 (SiPh), 127.2 (SiPh), 136.1 (SiPh), 153.0 (SiPh-*ipso*). $^{29}\text{Si}\{^1\text{H}\}$ NMR (54 MHz, 23 °C, benzene- d_6): δ 213.1 (d, $J_{\text{P-Si}} = 19.2$ Hz). IR (KBr, cm^{-1}): 3048, 2960, 2898, 1593 ($\nu(=\text{C}=\text{C})$), 1474, 1425, 1376, 1300, 1279, 1260, 1227, 1083, 1026, 945, 782, 732, 710, 650. Anal. Calcd for $\text{C}_{39}\text{H}_{57}\text{PRu}_2\text{Si}_2$: C, 57.46; H, 7.05. Found: C, 57.67; H, 7.39.

Acknowledgment. This research was partly supported by fellowships of the Japan Society for the Promotion of Science for Japanese Junior Scientists. We thank Dr. Masako Tanaka for assistance with the X-ray structure determination. We also acknowledge Kanto Chemical Co., Inc., for generous gifts of pentamethylcyclopentadiene.

Supporting Information Available: Details of the simulation for the VT-NMR studies of **3b-syn** and **3c** and X-ray crystallographic data for **3c**, **4a**, **b**, **5**, and **8a**, **c**; X-ray data are also available as electronic CIF files. This material is available free of charge via the Internet at <http://pubs.acs.org>.

OM030429+